Enhanced net CO_2 exchange of a semideciduous forest in the southern Amazon due to diffuse radiation from biomass burning

Simone Rodrigues[1,*], Glauber Cirino[1,4,5,*], Demerval Moreira[2], Andreae Pozzer[3], Rafael Palácios[4,5], Sung-Ching Lee[6], Breno Imbiriba[4], José Nogueira[†], Maria Isabel Vitorino[1,4], and George Vourlitis[7,*]

[1]Programa de Pós-Graduação em Ciências Ambientais, Universidade Federal do Pará, Belém-PA, Brazil
[2]Faculdade de Ciências, Universidade Estadual Paulista, Bauru-SP, Brazil
[3]Atmospheric Chemistry Department, Max Planck Institute for Chemistry, Mainz, Germany
[4]Instituto de Geociências, Faculdade de Meteorologia, Universidade Federal do Pará, Belém-PA, Brazil
[5]Programa de Pós-Graduação em Gestão de Risco e Desastre na Amazônia, Universidade Federal do Pará, Belém-PA, Brazil
[6]Department Biogeochemical Integration, Max Planck Institute for Biogeochemistry, Jena, Germany
[7]Department of Biological Sciences, California State University, San Marcos, CA, USA
[*]These authors contributed equally to this work
[†]Deceased
Correspondence: G. Vourlitis (georgev@csusm.edu)

Abstract. Carbon cycling in the Amazon fundamentally depends on the functioning of ecosystems and atmospheric dynamics, which are highly intricate. The radiative effects of aerosols on the Amazon-Cerrado biomes still need to be discovered for a wide variety of vegetation, usually unconsidered since that was not inventoried in previous studies. This study examines the effects of atmospheric aerosols on solar radiation and their effects on Net Ecosystem Exchange (NEE) in an area of

5   semideciduous tropical forest in the North of Mato Grosso State. Our results show that for a relative irradiance (f) 1.10-0.67, a decrease in incident solar radiation is associated with a reduction in the NEE. However, an average increase of 35-70% in NEE was observed when pollution levels Aerosol Optical Depth (AOD) were above ≈ 1.25 and $f < 0.5$. The increase NEE was attributed to the increase of up to 60% in the diffuse fraction of Photosynthetically Active Radiation. These results were mainly attributable to the biomass burning organic aerosols from fires. Important influences on Vapor Pressure Deficit (VPD)

10   and air Temperature (T_{air}) and Canopy (LC_T), induced by the interaction between solar radiation and high aerosol load in the observation area, were also noticed. On average, a cooling of about 3-4 °C and a decrease up to 2-3 hPa was observed for T_{air}, LC_T, and VPD, respectively. Given the long-distance transport of aerosols emitted by burning biomass, significant changes in atmospheric optical properties and irradiance will impact the CO_2 flux of semideciduous forests distributed in the region.

1   Introduction

15   Carbon (C) is a key element in global biogeochemical cycles, and understanding the biosphere-atmosphere fluxes of mass and energy is essential to understanding current and future terrestrial C storage. The role of Amazonian Forest ecosystems has been widely debated (Booth et al., 2012; Huntingford et al., 2013; Brienen et al., 2015), especially for Amazonian tropical forests (Doughty et al., 2015; Gatti et al., 2014, 2021). Redistribution of biomes and plant species (Davison et al., 2021), loss

of biodiversity (Brando et al., 2014; Saatchi et al., 2021), increase in fires (Brando et al., 2019; Alencar et al., 2022; Sullivan et al., 2020), outbreaks of pests and diseases (Anderegg et al., 2020) are examples of impacts, aggravated not only by climatic factors but also by anthropogenic ones (Ometto and Kalaba, 2022). These impacts have been threatening the largest pantropical CO_2 sinks since 1990'. Reductions from 1.26 PgC yr^{-1} to 0.29 PgC yr^{-1} are expected between 1990-2030, possibly reaching zero in the Amazon (Hubau et al., 2020). The result of increasing atmospheric CO_2 levels provides important feedback on the future of greenhouse warming (Booth et al., 2012; Huntingford et al., 2013). In the Amazon biome, forest ecosystems play an important role in terrestrial C storage, and while these forests seem to have a uniform behavior, there are distinct climatic sub-regions that affect C storage (Brienen et al., 2015; Gatti et al., 2021). CO_2 absorption through photosynthesis increases the vegetation and soil C stocks, representing a C sink, while plants, animals, microbial respiration, decomposition of dead vegetal biomass, and wildfires release CO_2, representing a C source to the atmosphere (Artaxo et al., 2022; Venturini et al., 2023; Silva Junior et al., 2020).

In general, the participation of forests in the global carbon cycle can only be adequately quantified by long-term studies monitoring C exchange at the plant-atmosphere interface. Forests are estimated to store 200-300 Pg C (Pan, 2011; Saatchi et al., 2011; Avitabile et al., 2016), about a third of what is contained in the atmosphere. This stock is very dynamic, and these trees process about 60% of global photosynthesis, sequestering about 72 Pg C from the atmospheric component through Gross Primary Production (GPP) every year (Beer et al., 2010) but releasing a similar amount back into the atmosphere from ecosystem (plant +animal+microbial) respiration (Nagy et al., 2018). With these large fluxes, a small proportionate change in CO_2 uptake or release can result in a large net C storage or sink. Carbon concentrations in the atmosphere have increased since the beginning of the industrial period and currently act with other C emission sources, such as the degradation of forests, mainly tropical ones. Recent reports (Gatti et al., 2021) show that some regions of the Amazon act as a source of CO_2 to the atmosphere, as a result of logging, land use change, and fires that occur in the region. However, regional numeric modeling (Moreira et al., 2017) and in-situ studies indicate (Carswell et al., 2002; von Randow et al., 2004) that Amazonian forests can occasionally be net atmospheric CO_2 sinks; or approximately in equilibrium (Vourlitis et al., 2011). In general, the balance between rates of carbon emission or carbon fixation is delicate, so small external disturbances can change the dynamics of the forest and the state of the climate system.

Among the modulating agents of the CO_2 balance, solar radiation is a fundamental component for both photosynthesis and respiration. In Brazil, and especially in the Amazon region, the biomass burning emits large amounts of gases and aerosols into the atmosphere, which can strongly alter radiative fluxes, impacting CO_2 flux (Aragão et al., 2018; Malavelle et al., 2019; Morgan et al., 2019; de Magalhães et al., 2019). Atmospheric aerosols from biomass burning affect ecosystem light use efficiency (LUE) and productivity, influence the amount and nature of solar radiation received in the system, and affect other environmental conditions such as temperature and humidity (Kanniah et al., 2012; Mercado et al., 2009). Studies of the effects of aerosols on terrestrial C cycling processes have found positive, negative, and neutral effects, and most of the research in the Amazon have been conducted in the central (Cirino et al., 2014), eastern (Doughty et al., 2010; Oliveira et al., 2007), and southwestern (Yamasoe et al., 2006; Cirino et al., 2014) parts of the basin. However, little research has been done on the ecotones in the Amazon, e.g., in the Cerrado-Amazonian Forest transition, which lies within the arc of deforestation, and other

biomes such as Cerrado-Caatinga, Cerrado-Atlantic Forests, and Pantanal forests. Numeric simulations have also demonstrated the impact of aerosols on GPP on the regional (Moreira et al., 2013; Rap, 2015; Bian et al., 2021) and global scales (Mercado et al., 2009; Rap et al., 2018), but physical representations of these impacts on transition ecosystems are still lacking. To our knowledge, this is the first study with this purpose.

The models, however, need improvements in parameterizing the radiative effects of aerosols and clouds on the NEE, e.g., a more realistic representation of the canopy structure and leaf physiological and morphological processes (Durand et al., 2021). Improvements in the aerosol optical model, its properties, secondary formation, lifetime, evolution, and absorption of aerosols are also critical (Drugé et al., 2022), especially those related to shape, size, and chemical composition. These improvements are fundamental for a more accurate and realistic spatial distribution of the atmospheric CO_2 absorption potential by Amazonian forests (Procopio et al., 2004; Moreira et al., 2017). In this sense, the potential for fire induced atmospheric aerosols to impact to CO_2 absorption by tropical semideciduous (seasonal) forests in Mato Grosso (in the arc of deforestation) has not been evaluated either by direct observation or numerical modeling. It is known that these forests play a central role in preserving biodiversity (Fu et al., 2018), are located on the frontier of deforestation, and experience seasonal variations in NEE (Vourlitis et al., 2011). These attributes make this region an excellent laboratory to assess the effects of atmospheric aerosols on forest NEE.

This research focuses on studying the action of biomass burning aerosols in an area of semideciduous forest located in the southern portion of the Amazon Basin, in the region the arc of deforestation of northern Mato Grosso, Brazil. To this end, we specifically seek to: (1) develop a clear-sky irradiance algorithm using a long observation period of Aerosol Optical Depth (AOD); (2) quantify the increase in the diffuse fraction of solar radiation due to the presence of aerosols from fires in the experimental study area; (3) quantify net and relative changes in NEE from changes in direct and diffuse radiation; and to (4) evaluate the influence of fires on biophysical variables that influence forest photosynthetic rates, such as leaf canopy temperature (LC_T), air temperature (T_{air}), and the vapor pressure deficit (VPD). Aerosol data and micrometeorological measurements with carbon fluxes measured by the eddy covariance system were used from 2005 to 2008. All solar radiation measurements are evaluated in terms of aerosol deph (AOD), solar zenith angle (SZA), and relative irradiance (f).

2 Materials and Methods

2.1 Site descriptions

The study area was located in the south of the Amazon basin, 50 km northeast of Sinop, in the municipality of Cláudia (Lat 11° 24.75' S, Long. 55° 19.50' W), in the State of Mato Grosso (Fig. 1). This forest is located in the arc of deforestation, a region of continuous agricultural expansion (areas for soybean and cattle pasture, logging, and fires) (Barbosa et al., 2023; Nepstad et al., 2014; Balch et al., 2015; Alencar et al., 2022) (Figs. S1, S2, and S3), and is recognized as seasonal, dry, or semideciduous forest (Ackerly et al., 1989; Ratter et al., 1978). Supplementary Figs. S3 and S4 show the study area different aerosol loads during the dry and rainy seasons, respectively. These figures were obtained from the time series of the Terra and Acqua Satellites (AOD$_m$, Table1).
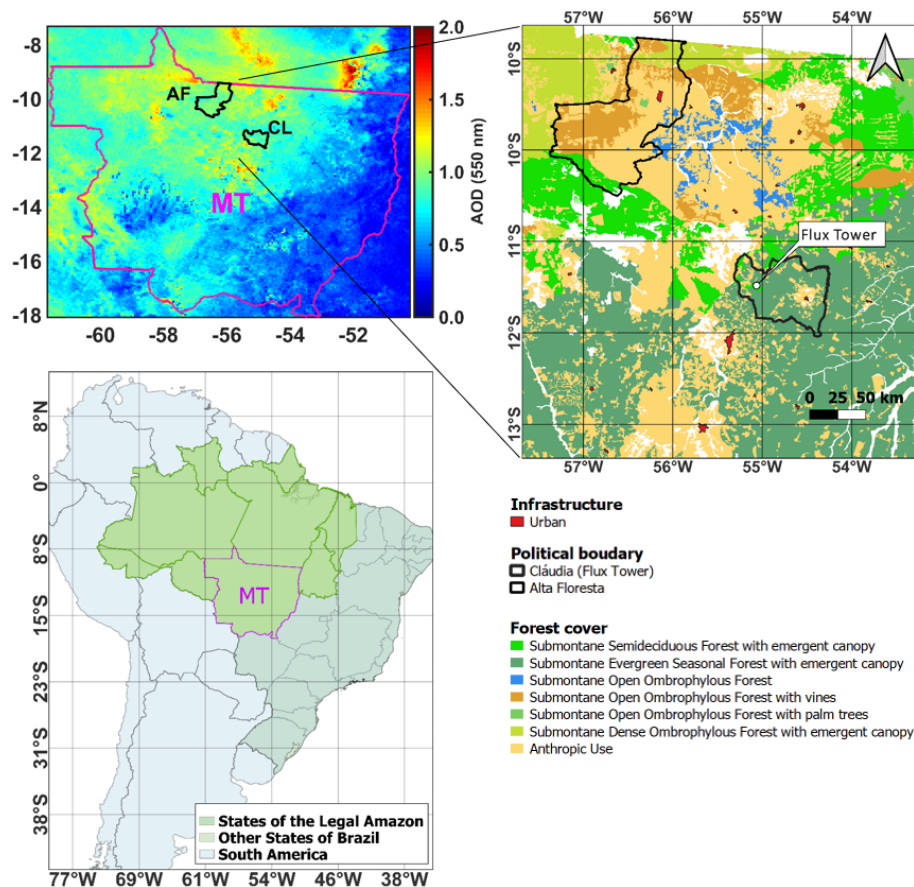
Figure 1. Localization map of a micrometeorological tower in the Cláudia municipality, 50 km northeast of Sinop, Mato Grosso (white point, in the right panel).

Previous studies report the characteristics of this type of forest (Vourlitis et al., 2011), which typically have trees with lower height, biomass, and floristic diversity compared to humid tropical forests (Murphy and Lugo, 1986; Nogueira et al., 2008) due to their well-defined seasonal variation in precipitation. The forest is 423 m above sea level, in a transition where the vegetation consists of Savannah (Cerrado), transitional vegetation (Cerradão), and Amazonian forest (Vourlitis et al., 2011).

The areas of transitional forests (Amazon Forest-Cerrado) covered approximately 41% (362,538 km^2) of the State of Mato Grosso. Due to the advance of the agricultural frontier, 21% of these areas suffered drastic reductions. Part of these forest areas are found in protected areas and territories of indigenous communities (approximately 17%). The deciduous and semideciduous forests of the Cerrado biome initially covered 49,951 km^2 in the State of Mato Grosso. Deforested areas represented $\approx 41\%$ of this total, with only 14% located in conservation units (Alencar A.; Nepstad D.; MacGrath D.; Moutinho, 2004). The geographic positions of these forests are discontinuous due to climatic fluctuations that have occurred in the last 10,000 years (Prado and Gibbs, 1993). Trees at this location are typical of the semideciduous forest of the Amazon, with maximum canopy

heights varying between 25-28 m. A comprehensive description of the species reported in the region was reported by Ackerly et al. (1989), Lorenzi (2000), and Lorenzi (2002). The soils are acidic with a pH measuring 4.2 and sandy (94% sand), well-drained quartzarenic neosols, poor in nutrients, and with low organic matter (Vourlitis et al., 2001; Oliveira-Filho AT and Oliveira, 2002), with a dry season that extends from May to September (Vourlitis et al., 2002). This area's 30-year average annual temperature is 24°C, with precipitation of approximately 2000 mm yr^{-1} (Vourlitis et al., 2002). The Bolivian High (BH) and South Atlantic Convergence Zone (SACZ) are among the active atmospheric systems in northern Mato Grosso, while southern Mato Grosso is affected by extratropical systems, such as Frontal Systems (Reboita et al., 2012). The loss of leaves (deciduousness) during the dry season (July-September) is sensitive to water availability and temperatures (maximum and minimum) in the region. With the arrival of the rainy season (November-May), trees that have lost their leaves begin to sprout again and produce new (Vourlitis et al., 2011).

2.2 Instrumentation and Data

2.2.1 Aerosol Measurements

This study used a long series of aerosol optical depth measurements – AOD (Aerosol Optical Depth) to assess the impact of atmospheric particles on the flux of solar radiation to the surface. Two types of remote sensors were used: the MODIS (Moderate Resolution Imaging Spectroradiometer) orbital sensor, available on board the AQUA and TERRA satellites, products MOD04-3K and MYD04-3K (Remer et al., 2013), and an AERONET (Aerosol Robotic Network) solar photometer, used as a standard measure of optical properties of atmospheric aerosols at the surface, between June1999-March2017 (Holben et al., 1998). All remote aerosol information required for this study was operated and maintained by NASA (National Aeronautics and Space Administration).

The TERRA /AQUA satellites have a heliosynchronous polar orbit, with a Local Time (LT) of passage over the study areas around 10h30min and 13h30min. These space platforms cover the Earth's surface every 1-2 days with radiance measurements in 36 spectral bands. The MOD/MYD043K aerosol products also feature the most current collection of data available from NASA, currently at 3 Km spatial resolution for AOD and other aerosol optical properties (Levy et al., 2013; Remer et al., 2013). Filters to exclude contamination of data by clouds are also applied during estimation processing. The AOD series from these satellites has 20 years of data on continents and oceans and is widely available on the open access platform of the Atmospheric Files Distribution System – Level 1, located at the Distributed Active Files Center (LAADS-DAAC) from Goddard Space Flight Center – GSFC, in Greenbelt, Maryland (USA). In this work, satellite AOD spatializations were used to obtain regional information on the nature or type of aerosol acting over the study area between 2000-2020 (Fig. S4). More detailed information about the MODIS sensor, such as spectral models, validation, and operating period of the aforementioned products can be found in Remer et al. (2005, 2013).

A long series of AOD measurements (> 20 years of data) are available for the city of Alta Floresta in northern Mato Grosso through CIMEL Electronique solar photometers, maintained and operated by NASA (GSFC), through the AERONET network (1999-2017). This photometer network is intended for the monitoring and characterization of aerosol particles in

various regions of the world. These sensors represent the standard measure of AOD and are widely used in the validation of satellite AOD estimates. The system operates solar radiation measurements and rotational interference filters to extract optical properties from aerosols in various spectral bands, between 340-1020 nm (Schafer et al., 2002b, a; Procopio et al., 2004; Schafer et al., 2008). This makes it possible to evaluate the direct influence of atmospheric particles in real time on regions highly affected by fires, such as the region of the arc of deforestation. In this work, AOD was used at wavelengths of 500 nm (AERONET) and 550 nm (MODIS). Both satellite and photometer data cover the entire period of micrometeorological and flux data, described in the next section. In the Alta Floresta, the AERONET system also has individual sensors and long-term measurements of incident shortwave solar radiation ($SW_i(t)$), as described in Table 1.

2.2.2 Micrometeorological Measurements

The CO_2 flux data set available for this research were widely used and cited by previous studies. Information regarding the systems installed in the micrometeorological tower is directly available in Vourlitis et al. (2011). An automatic weather station (ASW) to monitor the weather in the Cláudia municipality was used between Jun2005 and Jul2008. The implanted tower follows the standard of the micrometeorological measurement tower system of the Programa LBA (Nagy et al., 2016; Artaxo et al., 2022). In this research, the deployed tower consists of a pyranometer, thermometer, psychrometer, anemometer, pluviograph, and a turbulent vortex system (*eddy covariance*). Herein, these measures were used to represent the biophysical factors that affect the photosynthetic rates of forests. Micrometeorological data were measured every 30-60 s and stored by data-logger systems (CR5000) and (CR-10X), both Campbell Scientific, Inc., from which hourly averages were calculated (Vourlitis et al., 2011). The micrometeorological data set used in this work is the same used in the study prepared by Vourlitis et al. (2011), whose data are previously validated. Technical details such as precision, accuracy, and calibration can be found in Vourlitis et al. (2011); Moreira et al. (2017). All direct measurements used are listed in Table 1.

2.2.3 Measures of flux and concentration of CO_2

The eddy covariance system has been widely used to measure the net CO_2 flux by the ecosystem. This system performs measurements by correlation of turbulent vortices from a sonic anemometer and an infrared gas chamber (Infrared Gas Analyzer, IRGA), from which flux measurements of CO_2 (Carbon), water vapor (H_2O) and energy (sensible heat – H and latent heat – LE) are determined at high frequency, usually 10Hz. The data generated and recorded by the *eddy* system, deployed in flux towers, is normally adjusted by compilation software such as Alteddy 3.90 (Alterra, WUR, Netherlands). The carbon flux data from these micrometeorological towers are presented, using the classical sign convention in atmospheric science (negative flux indicates net ecosystem CO_2 uptake).

Table 1. List of measured variables and instrumentation used in the micrometeorological tower (at Cláudia Municipality) and AERONET station, in Alta Floresta. The *flags* [1], [2] and [3] indicate the instrumentation used in the flux tower, AERONET system and AQUA space platforms (TERRA), respectively.

Data set	Instrumentation		Attributes		
Measurements	Sensors [sites]	Models, Manuf.	Units	Symbols	Height
Inc. Solar Radiation	Pyranometer [1]	LI-200SB, LI-COR	Wm^{-2}	$SW_i(t)$	40.0 m
Photosyn. Active Rad.	Pyranometer [1]	LI-190SB, LI-COR	Wm^{-2}	PAR_i	41.5 m
Atmospheric Pressure	Barometer [1]	PTB101B, VSLA	hPa	P_{air}	42.5 m
Air Temperature	Thermohygrometer [1]	CS215, RMS	°C	T_{air}	41.5 m
Relative Humidity	Thermohygrometer [1]	HMP-35, VSLA	%	RH_{air}	41.5 m
Precipitation	Pluviometer [1]	GAUGE, MANUAL	mm	PRP	40.5 m
Wind Speed	Sonic Anemometer [1]	CSAT-3, CSCI	ms^{-1}	US_s	42.0 m
Wind Direction	Sonic Anemometer [1]	CSAT-3, CSCI	deg	US_d	42.0 m
CO_2 Flux	Eddy system [1]	LI-COR	$\mu mol\ m^{-2}s^{-1}$	FCO_2	42.0 m
CO_2 Vertical Profile	IRGA [1]	LI-820, LI-COR	ppm	$[CO_2]$	1-28 m
Inc. Solar Radiation	Pyranometer [2]	CM21, K&Z	Wm^{-2}	SW_{ia}	–
Aerosol Optical Depth	Photometer [2]	CIMEL	-	AOD_a	–
Aerosol Optical Depth	Modis-Terra [3]	MOD043K	-	AOD_m	–
Aerosol Optical Depth	Modis-Aqua [3]	MYD043K	-	AOD_m	–

2.3 Methods for calculating NEE and radiative effects of aerosols

2.3.1 Method to determine the net exchange of CO_2 in the ecosystem

The NEE is obtained from the eddy-covariance system. The eddy system provides CO_2 flux measurements at 10 Hz from a sonic anemometer (CSAT-3, Campbell Scientific, Inc., Logan, UT) integrated with an open-path gas analyzer (LI-7500, LI-COR Inc., Lincoln, NE). For NEE calculation, the storage term $S[CO_2]_p$ is obtained according to Aubinet (2012) and Araújo et al. (2010). For $S[CO_2]_p$ term calculation, we considered continuous measures of the CO_2 concentration vertically arranged between the ground and the top of the tower (Vourlitis et al., 2011). Under these conditions, the NEE of CO_2 is approximated by Equation 1:

$$NEE \approx FCO_2 + S[CO_2]_p \qquad (1)$$

where FCO_2 is called "CO_2 turbulent flux", calculated by the *eddy* system, above the treetops (Grace et al., 1996; Burba, 2013); $S[CO_2]_p$ is the vertical profile of the concentration of CO_2 or storage term (storage), considered a non-turbulent term measured at discrete levels z, at thicknesses Δz_i, from near the ground surface to the point of measurement of covariance of turbulent vortices in the tower (Finnigan, 2006; Araújo et al., 2010; Montagnani et al., 2018). In this work, the vertical profile $S[CO_2]_p$ was stratified into 5 reference levels (1, 4, 12, 20, and 28 m) (Vourlitis et al., 2011). Typical diurnal conditions consist of vector winds with speeds of 2.0 ms^{-1} and $u^\star \geq 0.20$ m s^{-1} and predominant SSW and SE directions. Approximately 72% of the

accumulated flux originates within 1 km and the representativeness of the measured CO_2 flux (footprint) is approximately 520 m (upstream of the tower), following the model proposed by Schuepp et al. (1990). The concentrations $[CO_2]$ were calculated following Aubinet et al. (2001) and Araújo et al. (2010), as reported by Vourlitis et al. (2011).

$$S[CO_2]_p = \frac{P_{air}}{RT_{air}} \int\limits_0^z \frac{\partial [CO_2]}{\partial t} \, dz \tag{2}$$

Where: P_{air} is the atmospheric pressure (Nm^{-2}), R is the molar constant of the gas ($Nm\ mol^{-1}\ K^{-1}$) and T_{air} the air temperature in degrees Kelvin (K).

We also calculated GPP from the NEE data and estimates of ecosystem respiration (R_{eco}) obtained from the nighttime NEE (see Supplemental information), however, relationships between the atmospheric optical properties and NEE were qualitative similar to those using estimated GPP (Fig. S11). Given the potential errors associated in estimating GPP and R_{eco} from the NEE data (Reichstein et al., 2005), we decided to use the measured values of NEE in our analysis of the impact of atmospheric aerosols on land-atmosphere CO_2 exchange.

2.3.2   Method to determine the solar irradiance of clear sky

The term clear sky was used here to designate the minimal influence of clouds and aerosols on the solar radiation measured by the pyranometer. To estimate the amounts of direct solar radiation to the surface under minimally overcast sky conditions, the measurements SW_{ia} of the AERONET 2.0 system observed under clear-sky (*cloudless*) conditions were used, that is, AOD $\leq$ 0.10 (Artaxo et al., 2022), lacking fire plumes. Under these conditions, we get Equation 3; a polynomial fit of order 4, here considered representative of the entire solar spectrum (Meyers and Dale, 1983). The model $S_0(t)$ obtained was used to derive the clear-sky instants at the surface (Fig. S7) between 07-17h (LT), according to the formulation below:

$$SW_{ia}\{AOD \leq 0.10\} \approx S_0(t) = at^4 + bt^3 + ct^2 + dt + e \tag{3}$$

Where $S_0(t)$ is the clear-sky solar irradiance as a function of time, in Wm^{-2}. The parameters (a, b, c, d, e) are the coefficients of the polynomial curve and t, the time, in local hours (LT). Figure 2 shows the mean diurnal cycle of the SW_{ia} obtained from long-term aerosol measurements by the AERONET system under different pollution conditions. The plot illustrates the sensitivity of the method applied to determine the expected irradiance levels on the canopy forest ($S_0(t)$) under varied atmospheric aerosol loads (AOD), C2, C4, and C6 curves. Markers C1, C3, and C5 represent averaged observations between 07:00-17:00 used to fit C2, C4, and C6 curves.

Our methods consider the cloud-screened database AERONET (Figure 2). Using the long series of measurements of AOD_a, it was possible to obtain different curves $S_0(t)$ for each month of the year, considering the seasonal variations of the SW_{ia} given in Equation 3. Figure S7 shows the seasonal variation of the $S_0(t)$ diurnal cycle throughout the year. The coefficients of the fit curves are listed in Table S1. To assess the consistency of the $S_0(t)$ model, obtained by SW_{ia} AERONET data set, we compared the outputs calculated by Equation 3 with the clear-skies solar irradiance model available by the Meteoexploration (SolarCalculator). The Solar-Calculator is a free system used to compute the clear sky solar irradiance, managed by Meteo
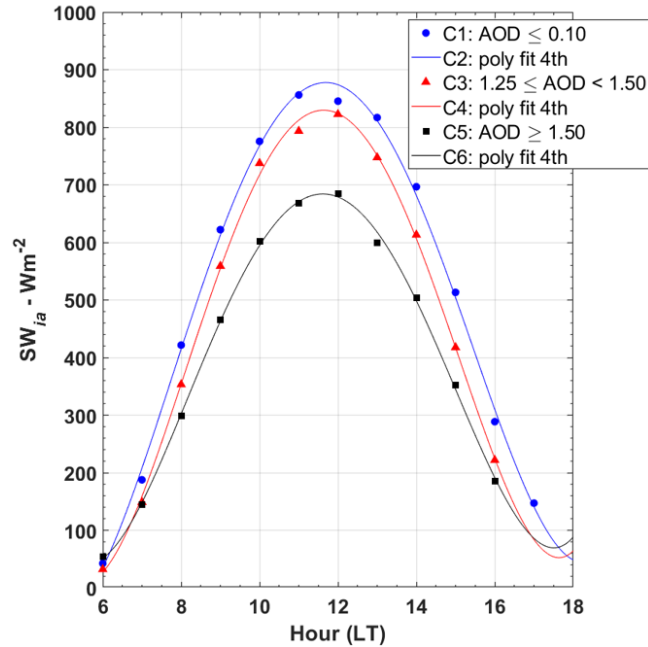
Figure 2. Incident solar irradiance under different sky conditions in Alta Floresta (June1997-March2017): clear-sky (C1 points and C2 curve, AOD ≤ 0.10) and polluted skies (C3 points and C4 curve, 1.25≤AOD≤1.50 C5 points and C6 curve, AOD>1.50)

205 Exploration company. The solar irradiance is calculated according to Bird, R. E., Hulstrom (1981), updated by Corripio (2003). The hyperlinked for Solar-Calculator is listed in Table S5. We also stated our algorithm is not accurate enough to separate shallow clouds of Biomass Burning Organic Aerosols plumes (BBOA). However, as the optical properties of deep clouds differ from aerosol (Machado et al., 2020), it is possible to distinguish them because the shading standard is notably different (Doughty et al., 2010). For example, deeper clouds often yield PAR(D)$_F$ ~ 1 (unit) meanwhile high loads of BBOA are usually

210 lower than < 1 (unit). In these conditions, the parameter f can be used as a sensible indicator of aerosol presence/entrance (Gu et al., 2003; Jing et al., 2010) but not to detect shallow clouds (translucent). In practice, the uncertainties for the radiative effects of aerosols on NEE are greater when PAR(D)$_F$ is near the unit. Thus, our algorithm cannot state the complete absence of clouds but is a crucial qualitative indicator of aerosols in the atmosphere when sunphotometers are not promptly available.

2.3.3 Determination of relative irradiance

215 In practical terms, the relative irradiance f expresses the relationship between incident solar radiation and that observed at the surface under a clear-sky (AOD ≤ 0.10) and cloudless (f ≥ 1.0). It is a parameter indicating the presence of pollution plumes with aerosols that scatter solar radiation and clouds, generally used in areas without direct instrumentation of clouds. This parameter has been considered a key indicator in the detection of clouds and plumes of pollution from fires in the Amazon Gu

et al. (2001); Oliveira et al. (2007); Cirino et al. (2014). To this end, the observed amounts of $\text{SW}_i(t)$ on the forest canopy are normalized by the irradiance $S_0(t)$, thus determining the quotient f (a dimensionless parameter), according to Equation 4. It is also highlighted that values of f can assume values as large as 1.2-1.3 ($f \sim$20-30%), typically due to the so-called "cloud gap effect" (Duchon and O'Malley, 1999; Gu et al., 2001). There is still no consensus on values in the literature about it. This term denotes the cloud-induced increase in surface irradiance. In general, there are multiple scatterings of solar radiation by the clouds around the study area, but still outside the Pyranometer's viewing angle. It will be seen in more detail in a few sections ahead.

$$f = \frac{\text{SW}_i(t)}{S_0(t)\{\text{AOD}_\text{a} \leq 0.10, \text{cloudless}\}} \tag{4}$$

Where $\text{SW}_i(t)$ is the total incident solar irradiance measured by the pyranometer (Wm^{-2}) under any atmosphere and $S_0(t)$ is the clear sky solar irradiance (Wm^{-2}) on a flat surface perpendicular to the sun's rays, without the attenuating effects of the atmosphere (clouds and burned) for a given time and place, ie $\text{AOD}_a \leq 0.10$ (*cloudless*). Values close to zero represent cloudy and/or smoky-sky conditions, and values close to unity represent clear-sky conditions (Gu et al., 1999; Oliveira et al., 2007; Jing et al., 2010; Cirino et al., 2014; Gao, 2020).

Here, we used f as a basis for comparison to detect the joint presence of clouds and aerosols from fires over the study area since the experimental site does not have instrumentation for direct observation of cloud cover. Obtaining this parameter is extremely important because when using clear-sky solar radiation as a base, solar radiation measured under overcast skies becomes a new metric for observing cloudiness. This variable will be compared with the NEE to assess the photosynthetic responses of the ecosystem to variations in the external environment.

2.3.4 Determining the clarity index

To determine the brightness index kt the extraterrestrial solar irradiance S_{ext} was first calculated depending only on orbital parameters. The index kt is a coefficient of proportionality between the measurements of direct solar radiation to the surface and S_{ext} and expresses the direct solar radiation transmitted in the atmosphere (Gu et al., 1999; Cirino et al., 2014). In a first approximation, kt indicates the transmissivity; the degree of transparency of the atmosphere to solar radiation at a given time and place, while f is a parameter of comparison more sensitive to the presence of radiation-scattering aerosols and clouds. Here, kt and SZA were used as predictors of the diffuse component of radiation (Gu et al., 1999; Cirino et al., 2014). For the calculation of the irradiance S_{ext} some parameters and variables are also needed such as the solar constant of the Earth (S_{ext}^t), the latitude of the location (φ), solar declination (δ), hour angle (h) and mean square distance between the Earth and the Sun (Gates, 1980). The determination of S_{ext} takes into account the angle of incidence of the solar rays and, therefore, the variations in the amounts of solar radiation at the surface, modulated by the SZA. Under these conditions, kt can be expressed according to Equation 5:

$$kt = \frac{\text{SW}_i(t)}{S_{ext}} \tag{5}$$

Where $SW_i(t)$ is the short wave radiation (Wm^{-2}) measured by the pyranometer (Table 1) and S_{ext} the extraterrestrial solar irradiance (Wm^{-2}) estimated on a perpendicular surface to the sun's rays, without the attenuating effects of the atmosphere for a given time and place, expressed according to Equation 6:

$$S_{ext} = S_{ext}^T \left(\frac{\bar{D}}{D}\right)^2 \times cos(z) \tag{6}$$

In this equation S_{ext}^t is the Earth's solar constant (≈ 1367 Wm^{-2}), $\bar{D}$ is the average earth-sun distance ($\sim 1.49 \times 10^6$ km), D is the earth-sun distance on a given Julian day, and cos (z) in the cosine of the solar zenith angle (SZA), calculated as proposed by Bai et al. (2012). This calculated index was used to establish the diffuse solar radiation, as described in detail in the next section.

2.3.5 Determination of diffuse PAR radiation

To determine the Diffuse component of the total PAR ($PAR(D)$), we adopted the procedures of Spitters et al. (1986) and Reindl et al. (1990), widely used in the literature when there are no direct measurements of radiation $PAR(D)$ (Gu et al., 1999; Jing et al., 2010; Zhang et al., 2010; Bai et al., 2012). The detailed calculation can be found in the one performed by Gu et al. (1999). The estimate is performed by deriving the diffuse PAR radiation according to the formulation below (Spitters, 1986).

$$PAR(D) = \left[\frac{1 + 0.3\left(1 - q^2\right)q}{1 + \left(1 - q^2\right)\cos^2\left(90 - z\right)\cos^3\left(z\right)}\right] \times PAR_i \tag{7}$$

Where $PAR(D)$ is the incidence of the diffuse (total) PAR (μmol photon m^{-2}s^{-1}), in the near-infrared range, in a horizontal plane to the Earth's surface, while q is a coefficient of proportionality used to denote the ratio of the total diffuse radiation to a given amount of irradiance (SW_i) at the surface given the sky conditions (Wm^{-2}). The parameter q is expressed considering ranges of variation for the index kt (Gu et al., 1999). To express the diffuse fraction of PAR radiation ($PAR(D)_F$) we use the relationship between $PAR(D)$ and PAR_i (Spitters et al., 1986). In the absence of direct measurements of diffuse solar radiation, the procedures reported by these authors are still widely used (Jing et al., 2010; Cirino et al., 2014; Moreira et al., 2017).

2.3.6 Determining the efficiency of light use

Another important parameter in this study is the light use efficiency (LUE), which expresses the efficiency of light use in photosynthetic processes by the canopy and is defined as the ratio between NEE and PAR_i. Several other procedures have been used to approximate the LUE; some use the coefficient of proportionality between the NEE and the $PAR(D)$ (Moreira et al., 2017) radiation, and others use temperature measurement directly on the leaf of the trees (LI-COR) to capture the photosynthetic response as a function of the variation in light intensity (Doughty et al., 2010). Canopy radiative transfer codes with validated physical parametrization for different leaf types are also used (Mercado et al., 2009). Here, for practical reasons,

we used the procedures applied by Jing et al. (2010) and Cirino et al. (2014), according to Equation 8, where LUE is given in percentage values.

$$LUE \cong \frac{NEE}{PAR_i} \tag{8}$$

We also performed the same procedure with GPP, but as mentioned above our results with GPP were qualitatively similar to those obtained using NEE. Since NEE was measured directly with only assess LUE calculated from NEE.

2.3.7 Determining leaf canopy temperature

We used the parameterization proposed from (Tribuzy, 2005) to estimate leaf canopy temperature (LCT) obtained from field experiments carried out in central Amazonia, 60-70 km NW from the center of Manaus-AM. Thermocouples temperature measurements on leaves provided a significant statistical relationship between PAR_i and RU_{air} during both dry (July-August/2003) and wet seasons (December 2003 to February 2004). The final equation obtained is expressed as a function of relative air humidity (RH_{air}) and radiation (PAR_i), valid for dry and wet seasons (Equation 9).

$$LC_T = [(2.48 \cdot 10^{-6}(RH_{air})^2 - 1.82 \cdot 10^{-4}(RH_{air}) - 1.83 \cdot 10^{-6}(PAR_i) + 0.0363)]^{-1} \tag{9}$$

Where LC_T is leaf temperature of canopy (°C), PAR_i and RU_{air} are photosynthetically active radiation (μmol m^{-2}s^{-1}) and relative humidity (%), respectively. Due to uncertainties and limitations underlying Equation 9, we also used an alternative method based on the Stefan-Boltzmann equation (Equation S1), following Doughty et al. (2010) and Cirino et al. (2014) (Figs. S9 and S10), results discussed in subsection 3.7.

2.3.8 Determination of clear sky NEE

The NEE observed on clear days (AOD < 0.1 and clear) was also used as a basis for comparing days with high aerosol loading. The Fig. 3 illustrates the behavior of the NEE under clear sky conditions ($f \approx 1.0$) between 07-17h (LT). The obtained polynomial fits are used to determine the $NEE_0(sza)$ as a function of SZA variations for each month of the year between Jun./2005 and Jul./2008 (Figure 3). We listed the curve coefficients in Table S2. The estimated curves and their goodness of fit are consistent with the behavior observed in previous studies (Gu et al., 1999; Cirino et al., 2014). We have used Equation 10 to estimate the $NEE_0(sza)$ throughout the year, considering the seasonal changes of biophysical factors such as solar radiation, deciduousness, water, and heat stress, that may add time-dependent noise to the fitted model. Figure S8 shows seasonal changes on the $NEE_0(sza)$ (hourly mean cycle).

$$NEE_0(sza) = p_1 SZA^2 + p_2 SZA + p_3 \tag{10}$$

Where $NEE_0(sza)$ is the NEE typically found on clear sky days (μmol m^{-2}s^{-1}). The parameters p_1, p_2, and p_3 are the coefficients of the polynomial curve and equal 0.0038, $-$ 0.99, and $-$ 12, respectively.

Like f, %NEE was used here as a basis for comparison for the maximum negative values observed during the study period, assuming the absence of water stress and nutrient deficiency (Gu et al., 1999; Oliveira et al., 2007; Doughty et al., 2010; Cirino et al., 2014).
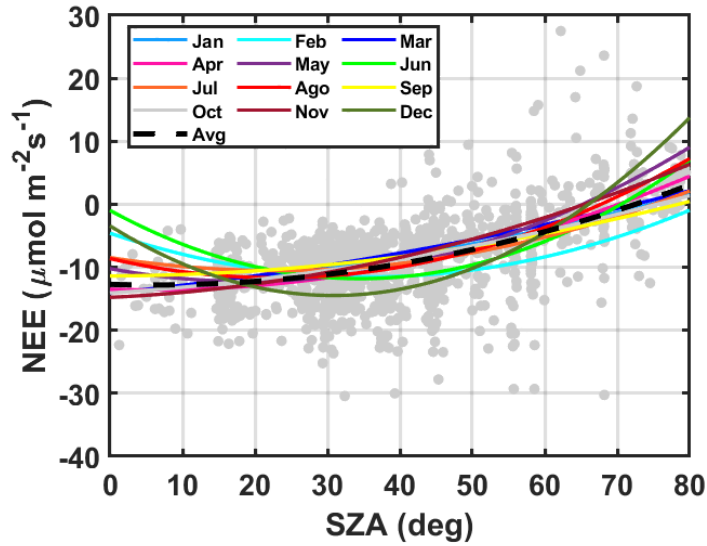
Figure 3. Show the NEE monthly changes as a SZA function to clear-sky conditions ($f \sim 1.0$) from 07 to 17h (LT), between Jun2005-Jul2008. Fitted curves coefficients $NEE_0(sza)$ were listed in Table S2. The black dot line is the annual average curve $NEE_0(sza)$.

Changes in observed NEE versus NEE under clear sky conditions were used to determine the percentage effect of aerosols on NEE. The $\%NEE$ was calculated by the following relationship (Bai et al., 2012; Gu et al., 1999; Oliveira et al., 2007):

$$\%NEE = \left(\frac{NEE(sza) - NEE_0(sza)}{NEE_0(sza)} \right) \times 100 \tag{11}$$

To eliminate solar elevation angle interference in the analysis of changes in $\%NEE$ versus f, we grouped the data into SZA ranges of 20-25°. This interval was small enough to minimize the effects of solar uplift during the day and to represent changes in NEE as a function of f in response to aerosols and/or clouds alone. This interval also ensured sufficient sample size for statistical analyses. SZA intervals smaller than 15° significantly reduced the sample size, making it impossible to develop a robust statistical analysis (Gu et al., 1999). Values above 50 or around 0 (solar angles very close to the horizontal and vertical plane, respectively) were generally very contaminated by clouds (Gu et al., 1999; Cirino et al., 2014).

2.4 Data analysis procedures

Computational routines were developed for compilation, certification, organization, and analysis of the variables presented in Table 1. We performed fitting curves and mathematical or statistical calculations with the packages available in MATLAB (2013). For data quality control, non-physical values outside acceptable levels were excluded from the database, totaling a loss of 3% of the total set of valid measurements (approximately 3,600 sampled points). We exclude unexpected maximum and minimum values for the region, e.g., values below and above 20-40°C, 40-95%, -40-40 (μmol m^{-2}s^{-1}), 0-1000 (Wm^{-2}) and

Table 2. List of indirect (calculated) variables, symbols, and measurement units of derived quantities, according to the cited body of literature.

Indirect Measures	Symbols	Units	Literature
CO_2 Net Exchange	NEE	μmol m^{-2}s^{-1}	Vourlitis et al. (2011)
Gross Primary Productivity	GPP	μmol m^{-2}s^{-1}	Wutzler et al. (2018)
Ecosystem Respiration	R_{eco}	μmol m^{-2}s^{-1}	Wutzler et al. (2018)
Vapour Pressure Deficit	VPD	hPa	Vourlitis et al. (2011)
Clear Sky Solar Irradiance	$S_0(t)$	Wm^{-2}	(Author)
Solar Zenith Angle	SZA	Degrees	Bai et al. (2012)
Relative Irradiance	f	-	Cirino et al. (2014)
Clarity Index	kt	-	Gu et al. (1999)
Extraterrestrial Solar Irradiance	S_{ext}	Wm^{-2}	Gu et al. (1999)
Diffuse PAR Radiation	$PAR(D)$	μmol phot. m^{-2}s^{-1}	Gu et al. (1999)
Diffuse PAR Fraction	$PAR(D)_F$	-	Gu et al. (1999)
Efficiency of Light Use	LUE	-	Jing et al. (2010)
Leaf Canopy Temperature	LC_T	°C	Tribuzy (2005)
Clear Sky NEE Exchange	$NEE_0(sza)$	μmol m^{-2}s^{-1}	(Author)
Relative NEE Exchange	$\%NEE$	%	(Author)

325   0-3000 (μmol m^{-2}s^{-1}) for T$_{air}$, RH$_{air}$, FCO$_2$, SW$_i(t)$, and PAR$_i$, respectively. Data analysis consists of three fundamental steps: (1) variation of solar radiation with optical depth AOD$_a$ analyzed as a function of irradiance f; (2) effects of aerosols and clouds on the net exchange of CO_2 at the forest-atmosphere interface and, finally, (3) quantification of photosynthetic performance as a function of pollution loads, and analysis of how pollution loads affected biological critical or optimal values for environmental factors such as T$_{air}$, LC_T and VPD (Vapour-Pressure Deficit). Photosynthetic performance, in all cases, is

330   analyzed as a function of NEE. In the end, the net percentage variation of the photosynthetic activity of the forest ($\%NEE$) is evaluated as a function of the irradiance f. Non-linear regression was used to determine functional relationships between NEE and other radiation variables. The relationships found are evaluated from the Poisson correlation and tabulated in terms of basic descriptive statistical parameters such as coefficient of determination (R^2) and significance level (P$_{value}$) with confidence intervals of 95%. Basic descriptive statistics are also applied to the data to obtain mean values, medians, percentiles, and

335   standard deviations for the measured and estimated variables. Table 2 lists indirect variables, calculated from the dataset listed in Table 1.

3 Results and Discussions

3.1 Average daily cycle of net exchange of CO_2

The average daily pattern of NEE observed in 2005-2008 (Fig. 4) follows the typical pattern of tropical forests (Gu et al., 1999; Niyogi et al., 2004; von Randow et al., 2004; Araújo et al., 2010; Vourlitis et al., 2011). Figure 4 shows maximum negative fluxes average -13.7 ± 6.2 μmol m^{-2}s^{-1} around 10-11h (LT), and the maximum positive fluxes average $+6.8 \pm 5.8$ μmol m^{-2}s^{-1} during the night period between 19h and 05h (LT). We observed a slight difference in the pattern of the daily cycle of the NEE between the wet and dry seasons (Fig. 4), with shift (an advance) in the peak absorption of CO_2 from the wet-to-dry season, from about 12h (LT) to 10h (LT), respectively (Fig. 4). Our estimates of CO_2 absorption were about 10-15% lower (i.e, less negative) during both seasons (< 0.6 μmol m^{-2}s^{-1}) when compared to Vourlitis et al. (2011). We hypothesize seasonal variations in water availability, nutrients, radiation, temperature, VPD, and pollution are counterbalanced throughout the year, producing an average seasonal behavior without significant differences in NEE.

Furthermore, different approaches in both studies can also explain the differences, i.e., analyses performed on different time scales. For example, (Vourlitis et al., 2011) reported average NEE of CO_2 values from daily and monthly time series. Similar monthly variations, with more negative magnitudes during the day in the rainy months (-9.0 μmol m^{-2}s^{-1} between November-February) and less negative during the light hours in the dry months (-7.7 μmol m^{-2}s^{-1} between May-August) were observed. The general balance of NEE revealed net carbon uptake of -0.12 μmol m^{-2}s^{-1} and -0.18 μmol m^{-2}s^{-1} during the wet and dry seasons, respectively. The maximum rates of photosynthesis and leaf canopy respiration were observed in October-November, which are the first months of the rainy season.
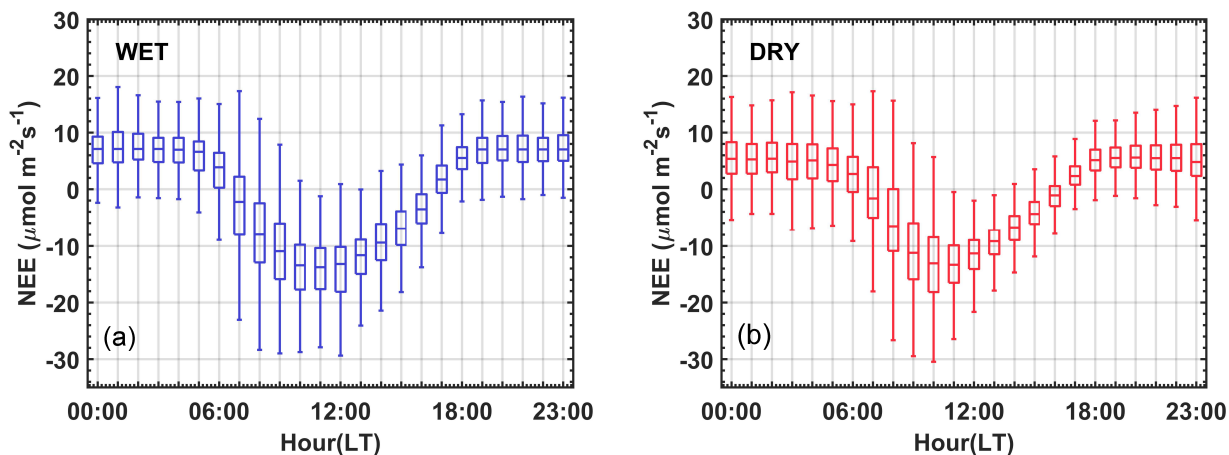
Figure 4. NEE average hourly cycle between June/2005 and July/2008, during the rainy (a) and dry (b) seasons for the semideciduous forest at the Claudia municipality. No filters are applied. The NEE is presented for any sky conditions during the year. The standard deviation is shown as vertical bars.

 3.2 The influence of aerosols on short wave solar radiation

The impact of aerosol particles by fires on the SW_i flux is evaluated as a function of f, AOD_a, SZA, $PAR(D)_F$ and PAR_i. Fig. 5 (a) shows the behavior of the relative irradiance f for different levels of AOD_a pollution, in the SZA ranges between 20-50°. A close and statistically significant relationship between f and AOD_a is observed with p-value < 0.01 and a coefficient of determination $R^2 \approx 0.92$ (Table 3). An approximately linear relationship is observed in which f decreases by about 40-60% when the AOD_a varies from 0.10 to 5.0, and no statistically significant difference was observed between mornings and afternoons. There is only a slight increase of $\approx$ 5-20% (on average) in the value of f between late mornings and afternoons, attributed here to the multiple scattering of solar radiation due to the formation of clouds near the tower (Gu et al., 2001). For SZA angles between 20 and 50°, there is a strong reduction in SW_i (225 ± 50 Wm^{-2}) associated mainly with the increase in the concentration of aerosols emitted by local fires or transported regionally during the burning season. Oliveira et al. (2007) and Cirino et al. (2014) reported results about 2-3 times lower for 20-30% reductions in f and AOD increase from 0.1 to 0.8, in FLONA-Tapajós (Santarém-PA) and central Amazon (K4), in Manaus-AM.
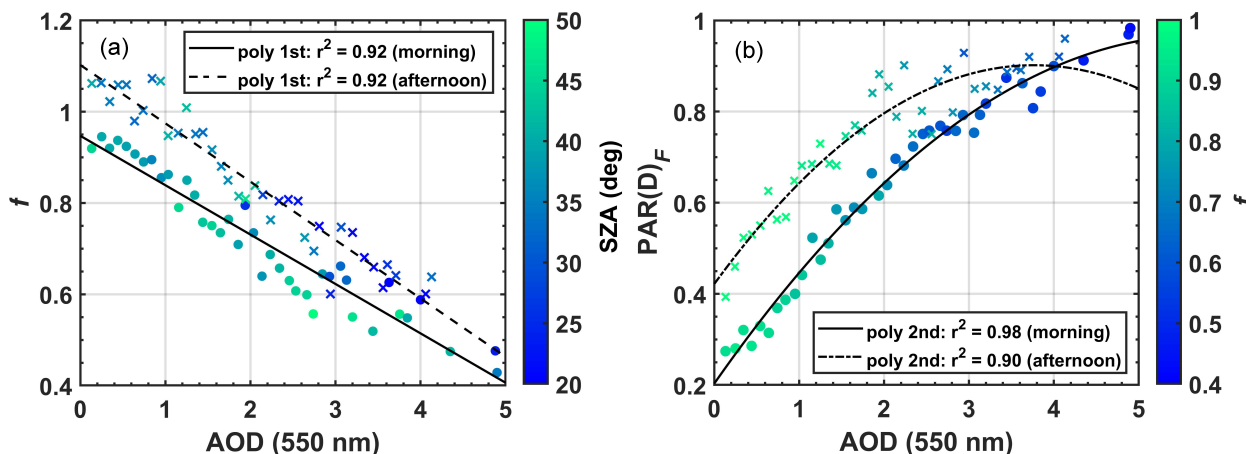
Figure 5. 3D-correlation between f and $PAR(D)_F$ with increasing AOD_a for different values SZA (a) and irradiance f (b) in semideciduous forest in the Cláudia municipality, 50 km northeast of Sinop-MT (2005-2008). Means are presented as clustered (bin) points, quantified, and determined in terms of standard deviation (STD) for each bin (STD shown in Table 3).

Figure 5 (a) shows the fraction of diffuse radiation calculated as a function of AOD_a, with a close statistical relationship observed ($R^2 = 0.98$ and 0.96) for the morning and afternoon hours (Table 3). Due to the reduction in the instantaneous fluxes of SW_i an increase of about up to 85% in diffuse radiation is observed when the AOD_a increases from 0.10 to 5.0. These results are consistent with previous studies carried out in the Brazilian Amazon (Doughty et al., 2010; Cirino et al., 2014; Rap, 2015; Moreira et al., 2017; Malavelle et al., 2019; Bian et al., 2021) and around the world (Niyogi et al., 2004; Jing et al., 2010; Rap, 2015; Rap et al., 2018) and proves to be particularly important due to to the ability of $PAR(D)$ to penetrate more efficiently into the leaf canopy, and under certain conditions, increase ecosystem in carbon uptake.

Table 3. Polynomial adjustments (Fig. 5), coefficients and statistics for the morning and afternoon periods in the micrometeorological tower in Cláudia-MT (2005-2008). R^2 is the correlation coefficient, $\Delta\mathbf{SW}_i$ is the incident shortwave radiation amount, and STD is the Standard Deviation.

Settings		Period	Coefficients			Statistics	
Polynomial Functions		Local Hours	a	b	c	R^2	$\Delta\mathbf{SW}_i$ (STD)
f	poly fit 1st	07-12h	-0.11	0.95	–	0.92	-200 ($\pm$ 50)
	–	12-17h	-0.13	1.10	–	0.92	-250 ($\pm$ 80)
$PAR(D)_F$	poly fit 2nd	07-12h	-0.023	0.27	0.20	0.98	-97 ($\pm$ 30)
	–	12-17h	-0.034	0.25	0.42	0.90	-118 ($\pm$ 42)

3.3 The influence of aerosols on diffuse radiation

375 Figure 6 shows the behavior of PAR_i and $PAR(D)$ as a function of f and SZA. For reductions in f of $\approx 40\%$ (f ranging from 1.0 to 0.6) there were strong reductions in PAR_i ($\sim 750\ \mu$ mol m^{-2}s^{-1}) and a corresponding 55% increase in diffuse radiation $PAR(D)$ ($\sim 600\ \mu$mol m^{-2}s^{-1}) between July-December. These numbers indicate a strong reduction in PAR_i as pollution levels increase and change from clear sky conditions (AOD ≤ 0.10, $f \sim 1.0$) to aerosol smoky sky conditions of fires (AOD $\gg 0.1$, $f \ll 1.0$). Figure 6a shows a decreases almost linearly between PAR_i and f, meanwhile behavior $PAR(D)$

380 versus f is non-linear (Figure 6b). The polynomial fits, coefficients, and inflection points are displayed in Table 4. $PAR(D)$ reach maximum values (779-1080 μmol m^{-2}s^{-1}) for f between 0.63 and 0.66 (reductions of 37 %-34%) and ranges SZA (20-40°). The negative variations in f also suggest high pollution load for fires at the site (AOD $\gg 0.10$) producing statistically significant reductions of up to 35% in the PAR radiation flux (Figs. 6a and 5a) and a 50% increase in $PAR(D)_F$ (Figs. 6b and Fig. 5b).

385 For SZA $< 40°$, it is observed the higher variation rates PAR(D) f^{-1}, indicating the entrance/presence of plumes-pollution and clouds over the measurement tower's pyranometer. Table 4 shows a slight shift of the tipping points (Cp) towards smaller values of f ($\sim$1.0-0.60), as well as an accentuated increase in PAR(D) (50%, $\sim$400-500 μmol phot. m^{-2}s^{-1}). These results are likely linked to greater optical thickness of the atmosphere at the beginning and end of the day and higher aerosol concentration (BBOA). Here, we raised two reasonable hypotheses: (1) lower PBL (Planetary Boundary Layer) favors higher

390 BBOA concentration over the tree canopy, usually between 06-09h LT (SZA $< 75°$); (2) thicker PBL, provides deeper-clouds and higher shading on the canopy (Oliveira et al., 2020), beyond favors dispersion of fires Nepstad et al. (2014), intensifying BBOA concentration at local by advection or particle regional-transport (Figs. 1, S4-S6). For a given period of the year, under stable meteorological conditions, BBOA can explain changes in PAR(D), at least on an hour basis, especially between May and October, when evapotranspiration is more than rainfall (ET $>$ PRP) Vourlitis et al. (2002, 2011) and deeper cloud-cover

395 fraction is lower often. In the other months of the year, clouds and aerosols mix, producing radiative effects inseparable, considering our instrumentation and dataset available at the local studied. The 50% increase in $PAR(D)$ can be mainly attributed to radiation-scattering particles (BBOA), especially during the dry season (Shilling et al., 2018; de Sá et al., 2019) indeed
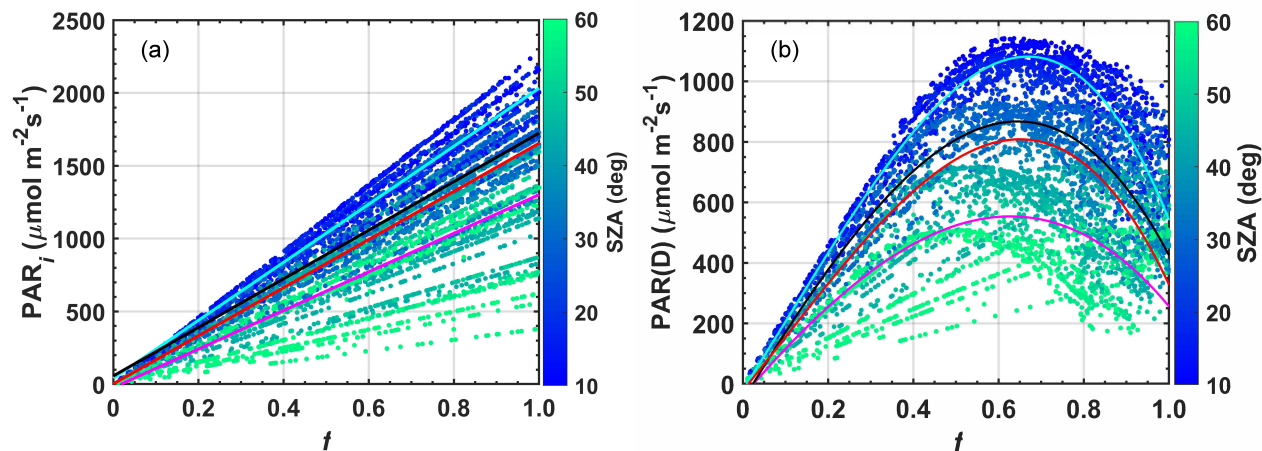
Figure 6. (a) 3D-correlation between f, PAR$_i$ (a) and $PAR(D)$ (b) for different SZA values. The blue, black, magenta and red lines are the polynomial curves adjusted to the analyzed SZA variation ranges, respectively equal to 0-20º, 20-40°, 40-60°, and 0-60º, in semideciduous forest in the Cláudia municipality, 50 km northeast of Sinop-MT (2005-2008).

Table 4. Polynomial adjustments (Fig. 6), coefficients, and statistics for the morning and afternoon periods in the micrometeorological tower in Cláudia-MT (2005-2008). **C**p (x_v, y_v) is the critical point of the fit curve, where the derivative is equal to zero.

Settings	Angles	Coefficients				Statistic	
Polynomial Functions	**SZA**	**a**	**b**	**c**	**d**	**R^2**	**Cp (x_v, y_v)**
PAR$_i$ poly 1st	0-20°	$+1.5 \times 10^3$	$+56$			0.92	
	20-40°	$+2.0 \times 10^3$	$+41$			0.86	
	40-60°	$+1.7 \times 10^3$	$+57$			0.64	
	0-60°	$+1.3 \times 10^3$	-23			0.67	
$PAR(D)$ poly 3rd	0-20°	-2.5×10^3	$+8.4 \times 10^2$	$+2.2 \times 10^3$	-19	0.92	(0.66, 1080)
	20-40°	-1.3×10^3	-5.6×10^2	$+2.3 \times 10^3$	-56	0.66	(0.63, 846)
	40-60°	-6.4×10^2	-7.0×10^2	$+1.6 \times 10^3$	-41	0.42	(0.61, 529)
	0-60°	-2.0×10^3	$+5.8 \times 10^2$	$+1.7 \times 10^3$	-22	0.40	(0.63, 779)

cloud-cover. On fire seasons, about 80% of BBOA is composed of fine particles PM$_{2.5}$ (Bian et al., 2021) from which 10% is BC (Black Carbon) and BCr (Brown Carbon), which both Single Scattering Albedo (SSA) and AOD can be affected. In general, these particles have the potential to heat the atmosphere (absorption greater than reflection), producing values that may be above the optimal physiological thresholds of the ecosystem, influencing CO$_2$ absorption rates (maximum-negative NEE). It is also possible a mix of other kinds of particles from long-range transport with complex chemical properties, e.g., urban aerosols and African BBOA (de Sá et al., 2019; Holanda et al., 2023).

400

3.4 The indirect effect of aerosols on the use of light efficiency by the forest

405   There was a well-defined monthly variation of AOD_a, as shown in the previous sections. Since fires are the main cause of changes in the physical and chemical composition of the atmosphere throughout the year (Martin et al., 2010b, a; Artaxo et al., 2013, 2022), statistically significant reductions were found for the SWi and PAR_i. This section mainly evaluates the optimal levels of PAR_i as well as the effects of changes in the efficiency of solar radiation use by the forest ($LUE \approx NEE/PAR_i$). The analyses are performed as a function of $PAR(D)$ radiation, from which the maximum efficiency of light use for the studied

410   semideciduous forest is determined. Under smoky sky conditions (AOD $\gg$ 0.10), carbon assimilation gradually increases with increasing PAR_i reaching maximum saturation around 1550 and 1870 μmol m^{-2}s^{-1} in the range between 20-50° SZA, values for which the maximum NEE (negative) is approximately -23 μ mol m^{-2}s^{-1}. Under clear sky conditions, considering the same SZA range, the maximum negative NEE is about around -18 μmol m^{-2}s^{-1}, which occurs with a PAR_i of 2100-2300 μmol m^{-2}s^{-1} (Fig. 7a). To complement this analysis, the LUE flux normalized by $PAR(D)_F$ during days with high aerosol

415   loading in the burning season (Fig. 7b). Under these conditions, the forest reaches maximum NEE fluxes on smoky days and not under clear sky conditions. The results reveal that smaller amounts of energy are needed for the forest to reach maximum saturation on non-polluted days. The analyses presented in Fig. 7 confirm greater photosynthetic efficiency under smoky sky conditions for the studied semideciduous forest ecosystem, results compatible with field observations (Oliveira et al., 2007; Doughty et al., 2010; Cirino et al., 2014) and by numerical modeling in the Amazon (Rap, 2015; Moreira et al., 2017; Malavelle

420   et al., 2019; Bian et al., 2021) and the world (Rap et al., 2018).
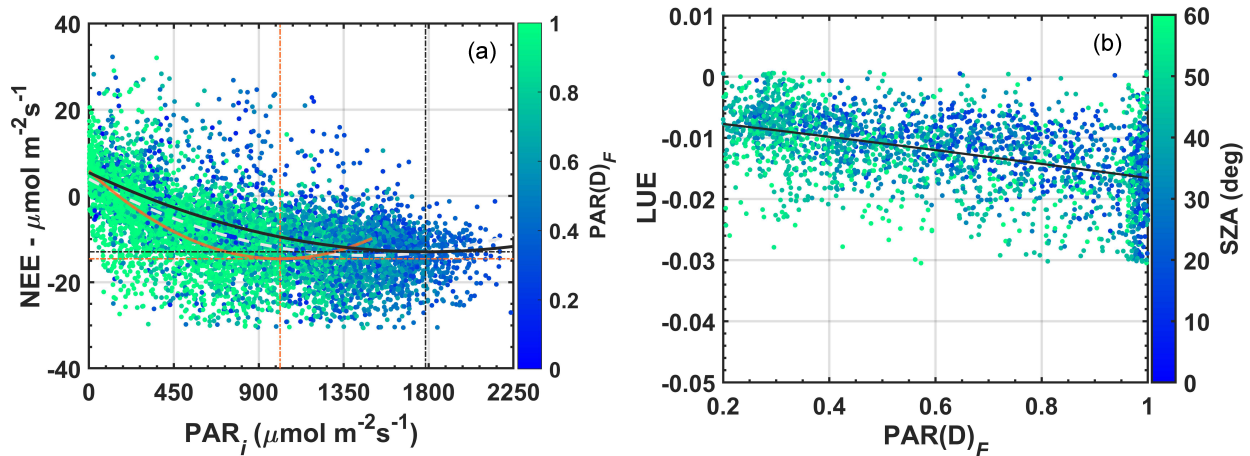
Figure 7. NEE as a function of radiation, PAR_i for measurements between 08h and 17h LT (a). In image (b) LUE is a function of the fraction $PAR(D)_F$ (R^2 = 0.21, the value of $p < 0.001$) for an area of semideciduous forest located in the municipality of Cláudia- MT, 50 km north of Sinop, between Jun2005-Jul2008. The orange and black lines denote, respectively, observations $PAR(D)_F \geq 0.60$ and observations $f \sim 1.0$ (clear-sky conditions). The orange and black vertical lines indicate the global minima of the polynomial curves.

Due to the physicochemical nature of the BBOA and its intrinsic properties (Cirino et al., 2018; Adachi et al., 2020), the radiation $PAR(D)$ affects the NEE and the functioning of several Amazon forest ecosystems (Rap, 2015; Rap et al., 2018; Bian et al., 2021), especially where tree species adapted to low light conditions occur, for example, in the leaf sub-canopy of Amazonian forests (Mercado et al., 2009).

425   Photosynthetic efficiency (LUE), closely linked to the canopy's ability to convert solar energy into biomass, is $\sim$ 1-2% for the studied forest, indicating loss or rejection of a large part of the solar energy available for photosynthesis. However, for high values of $PAR(D)_F$, close to 1.0, peaks of up to 3% in LUE are observed. In situations where the diffuse fraction total maximum values, the values of AOD_a are on average < 1.0 and $f \ll 1.0$. These findings corroborate the previous analyses and reinforce the presence of radiation-scattering aerosols emitted by the fires over the studied area. It is noteworthy that changes
430   in $PAR(D)_F$ (Fig. 7b) express proportional changes in $PAR(D)$.

Although there is great uncertainty (high standard deviation) in the behavior of LUE with increasing radiation $PAR(D)$, there is a gradual, approximately linear increase in the values of LUE in the range of radiation $PAR(D)_F$ between 0.20-1.0. This behavior is peculiar to tall vegetation with a generally leafy canopy of tropical forests, which are more sensitive to the transfer of $PAR(D)$ radiation from the top canopy to the bole. In short-stature vegetation, as in the semiarid region of northeast
435   China (e.g., grasses), the LUE remains approximately constant even for high values of $PAR(D)$ generated by aerosols and clouds (Jing et al., 2010). Overall, however, the LUE is low for many vegetation types, typically between 1-3%.

3.5   The net absorption of CO₂ due to aerosols from fires

Figure 8 shows the relative changes in the NEE during all months of the year, discounting confounding factors due to the seasonality, i.e., monthly changes of variables that strongly affect photosynthetic rates. Three essential reasons reinforce the
440   use of the whole year in these analyses: (1) wet season contains about 15-20% of the wildfires number detected during the dry season (Tab. S4). We observed numerous hotspots of fires around the area of the study, i.e., BBOA sources emitted locally and transported regionally (Fig. S5); (2) the relative contribution of BBOA during the wet season is relatively small but contributes to improving the sample space, considered a critical aspect to the study; (3) removing or maintaining transition and rainy periods in the analyses does not change the scientific direction of the results initially found in Figure 8b (see Figs. S12-13).

445   **3.5.1   Seasonality of biophysical factors on NEE**

To reduce the effect due to the seasonality of biophysical factors strongly driven by the change in weather conditions during the year (e.g., water stress, deciduousness, ecosystem respiration), we normalized Equation 11 by the clear-sky NEE adjusted to each month of the year (Fig. S8) shows average monthly changes found in the period 2005-2008). These adjustments better support our assumptions regarding the derived quantities described in the methods. In fact, we observed a relative average
450   increase of 30% on the $\%NEE$ to SZA ranging from 0-75° after applying these corrections, compared with a single curve for all years. To SZA ranging 0-20° um enhancement up to 70% on the $\%NEE$ was observed. Since many studies do not take these corrections into account, these results suggest that the impacts of BBOA on the NEE can be even more significant than
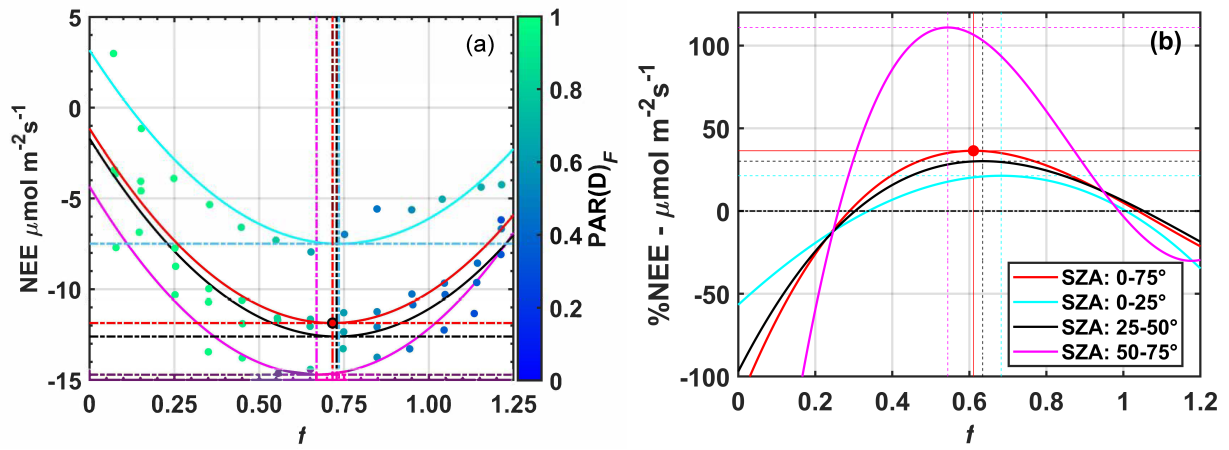
Figure 8. Variability of NEE with f for various SZA ranges in (a). The $\%NEE$ as a function of the irradiance f for the same SZA intervals is shown in (b). The $\%NEE$ is calculated from Equation 11, corrected with the $NEE_0(sza)$ computed from the fit curves presented in Table S2. These graphs include the effects of aerosols in the experimental area of Cláudia-MT, between 2005-2008

previously known, especially in the Central (Manaus, K34) and Western Amazon (Ji Paraná, RBJ) (Oliveira et al., 2007; Cirino et al., 2014; Rap, 2015; Moreira et al., 2017).

455   The Equation 11 and Equation 4 allowed us to evaluate the behavior of the ratio between the $\%NEE$ and the irradiance f for intervals SZA from 0-75°. This procedure was adopted to minimize the effects of solar elevation and air temperature on the NEE flux throughout the day (Gu et al., 1999; Cirino et al., 2014). The intervals every 25° ensured the smallest possible SZA variations and the largest possible number of points within the sample space necessary for statistical analyses. For each SZA interval analyzed, the average $\%NEE$ was evaluated in *bins* of f equal to 0.1, calculated separately (Fig. 8). The critical points

460   and the coefficients of curves for all data (between 0-75° SZA) are shown in the supplementary material (Fig. S12, Table S3). On average, an average (absolute) increase of approximately 7.0 μmol m^{-2}s^{-1} in carbon uptake was observed relative to clear sky conditions when f varied from 1.1-1.0 to 0.66, results for the SZA range between 0-75° (Fig. 8 (a)). The 7.0 μmol m^{-2}s^{-1} increase represents a 20-70% increase in NEE flux. This increase, strongly linked to the increase in aerosol concentration by fires, is mainly explained by the 50% increase in $PAR(D)_F$, ($\approx$ 450 μmol m^{-2}s^{-1} in the stream $PAR(D)$) and 35-40%

465   reduction in the irradiance f when the AOD$_a$ varies from 0.10 to 5.0, As it was shown in the Figure 5b).

Oliveira et al. (2007) and Cirino et al. (2014) showed a relative increase of about 30% for f values ranging from 1.1 to 0.80. These studies showed that the increase in carbon uptake in the presence of aerosols and clouds becomes smaller and similar in both locations for SZA bands < 20. Solar radiation suffers less scattering near the zenith ($SZA \sim 10°$) due to particles suspended in the atmosphere and the narrowing of the optical path, reducing the effects of diffuse radiation on the

470   photosynthetic process. These results, in particular, are repeated for the studied semideciduous forest of Mato Grosso, but a strong increase of 70% in $\%NEE$ is observed for lower SZA ranges (between 50-75%), in the early hours of the day, between 8-10h (LT), while in the Jaru Biological Reserve (JBR) the biggest increases are concentrated in the SZA ranges between

10-35°, close to midday, or in the morning-afternoon (Oliveira et al., 2007). At K34, in Manaus, the maximum absorptions and the maximum $\%NEE$ that occur do not exceed 20% and the effects of aerosols and clouds operate together. The individual radiative influences of clouds and aerosols are difficult to quantify because satellite AOD observations have a low temporal resolution. Similar results were observed by Doughty et al. (2010) in FLONA-Tapajós, central Amazon. In general, higher standard deviations are found in regions most heavily impacted by aerosols (Oliveira et al., 2007; Cirino et al., 2014; Rap, 2015), such as Ji-Paraná (RO) and Alta Floresta (MT). Because aerosol concentrations are relatively lower in FLONA-Tapajós (PA) and Manaus (AM), the standard deviations are lower (Oliveira et al., 2007; Doughty et al., 2010; Rap, 2015). Theses deviations can be found in previous studies published by Oliveira et al. (2007) in FLONA-Tapajós (PA), Cirino et al. (2014) in Manaus (AM), and Ji-Paraná (RO).

Table 5 lists the coefficients of the adjustments found for NEE and $\%NEE$ as a function of f for each of the SZA ranges considered. We identified the optimal and critical radiation conditions for carbon uptake between 07-17h (LT) and listed them below. As mentioned before, tipping points (C_p) represent the called physiological optimums. Our results show a substantial decrease (increase), significant statistically, of NEE ($\%NEE$) as a function of f from -7.5 μmol m^{-2}s^{-1} to -14.7 μmol m^{-2}s^{-1} and 1-0.63 ($\approx$40%) when SZA ranges from 0-25° to 50-75°, respectively ($R^2 \geq 0.85$).

Table 5. Polynomial adjustments (Fig. 8), coefficients, and statistics for the periods between 07-17h (LT) in the micrometeorological tower 50 km from Sinop-MT, in the municipality of Cláudia, between 2005-2008.

Settings	Angles	Coefficients				Statistic	
Poly fit 2nd	SZA	a	b	c	d	R^2	$Cp\,(x_v, y_v)$
NEE	0-25°	$+23$	-31	-4.3		0.88	(0.74, -07.50)
	25-50°	$+21$	-30	-1.7		0.95	(0.73, -12.61)
	50-75°	$+20$	-29	$+3.1$		0.88	(0.67, -14.71)
	0-75°	$+21$	-30	-1.1		0.97	(0.72, -11.90)
Poly fit 3rd	SZA	a	b	c	d	R^2	$Cp\,(x_v, y_v)$
$\%NEE$	0-25°	-3.5×10^1	-1.2×10^2	$+2.1 \times 10^2$	-5.7×10^1	0.89	(0.68, 21.31)
	25-50°	$+1.4 \times 10^2$	-4.9×10^2	$+4.6 \times 10^2$	-9.7×10^1	0.97	(0.63, 30.13)
	50-75°	$+1.1 \times 10^3$	-2.9×10^3	$+2.1 \times 10^3$	-3.8×10^2	0.96	(0.54, 110.9)
	0-75°	$+2.0 \times 10^2$	-6.6×10^2	$+5.8 \times 10^2$	-1.2×10^2	0.98	(0.61, 36.40)

These results correspond, respectively, to the relative increase ($\%NEE$) of about 25-110% in the first and last hours of the day, when the lower solar angles (greater physiological optimum), corroborated to results presented in Figure 5, Figure 6 and Table S4. For lower than 0.63, we also observed a strong decadent of photosynthetic rates until $f \sim 0.25$ when the photosynthesis process breaks altogether. Thus, $f \sim 0.66$ (SZA 0-75º) can be interpreted as a threshold for which photosynthetic

rates ($NEEf^{-1}$) indicate a strong reduction in the carbon uptake capacity of forest in response to overload BBOA. As for enhancements in the NEE, attributed to light-shading, it must be sighted as a narrow resilience of forest in response to a polluted atmosphere. These results offer more direct insight into alterations in solar radiation caused by BBOA and its impacts on carbon uptake during the day, although there are uncertainties not measured associated with clouds.

3.6 Insights into ecosystem-respiration uncertainties

Since no direct local measurements of Ecosystemic Respiration (R_{eco}) exist, estimates are necessary. However, typically, the models available in the literature grossly overestimate or underestimate the local R_{eco}, especially when in-situ data are unavailable to fit them (e.g., autotrophic and heterotrophic respiration; litter, soil, trunks, branches, leaves, and roots) (Malhi, 2012). It is important to highlight that the indirect effects of BBOA on R_{eco} were not exploited yet in the "Cerrado-Amazon Forest" ecotone. Little is known about how aerosols modify the R_{eco} in the region. We highlighted that previous studies by (Vourlitis et al., 2002, 2011) made daily estimates for the R_{eco} without isolating the radiation-attenuating effects due to aerosols. These conditions are pretty different for the current study. Once photosynthetic rates are also modulated by solar radiation (attenuated by BBOA), changes in the VPD may also be impacting ecosystem respiration from no-linear interactions, influencing the opening and closing of stomata, canopy temperature, humidity, and soil temperature. All these factors influence the microbiological dynamics of the soil and litter, with implications still unknown for R_{eco} (in-situ). Thus, we assume that the uncertainties underlying the calculation of the R_{eco} (for the reasons mentioned) could affect our results equally significantly by disregarding it. Therefore, we assumed $GPP \approx NEE$ on a monthly basis.

To better support our assumption ($GPP \approx NEE$), we have done a similar test (Figs. 8b and S12) using only daytime data during the dry season (Figs. S12 and S13). We found that the % change (on average) is similar, around 15% for SZA (0-75º) and around 35% for SZA (50-75º). Both differences may be attributed to uncertainties due to the daytime R_{eco} (Figure S11c) and factors that need to be better explored in future work. We hypothesized some mechanisms that could lead to an increase in NEE throughout the dry and smoky seasons (strongly supported by previous studies in the Amazon and world), as follows below. (1). During the dry season (Jul-Sep), photosynthetic deficit due to deciduality is partially compensated by positive feedback of extrinsic factors: BBOA concentration, $PAR(D)$, cooling of the air and leaf canopy, and VPD reduction (Vourlitis et al., 2001; Gu et al., 2003; Rap et al., 2018; Corwin et al., 2022). (2). During the flush new leaves season (Oct-May), photosynthetic enhancement is primarily explained by positive feedback both extrinsic (mentioned) and intrinsic factors (Leaf Area Index and LUE): variation in the characteristics of the forest canopy due to the newly sprouted leaves, i.e., higher photosynthetic capacity of canopy that compensates the unfavorable stomatal response due to precedent drought (Wu et al., 2016; Green et al., 2020); (3). The magnitude of the effects observed in assumptions (1) and (2) will strongly depend on the intensity and frequency of occurrence of meteorological phenomena (e.g., planetary limited layer dynamics) (Fuentes et al., 2016; Gao, 2020).
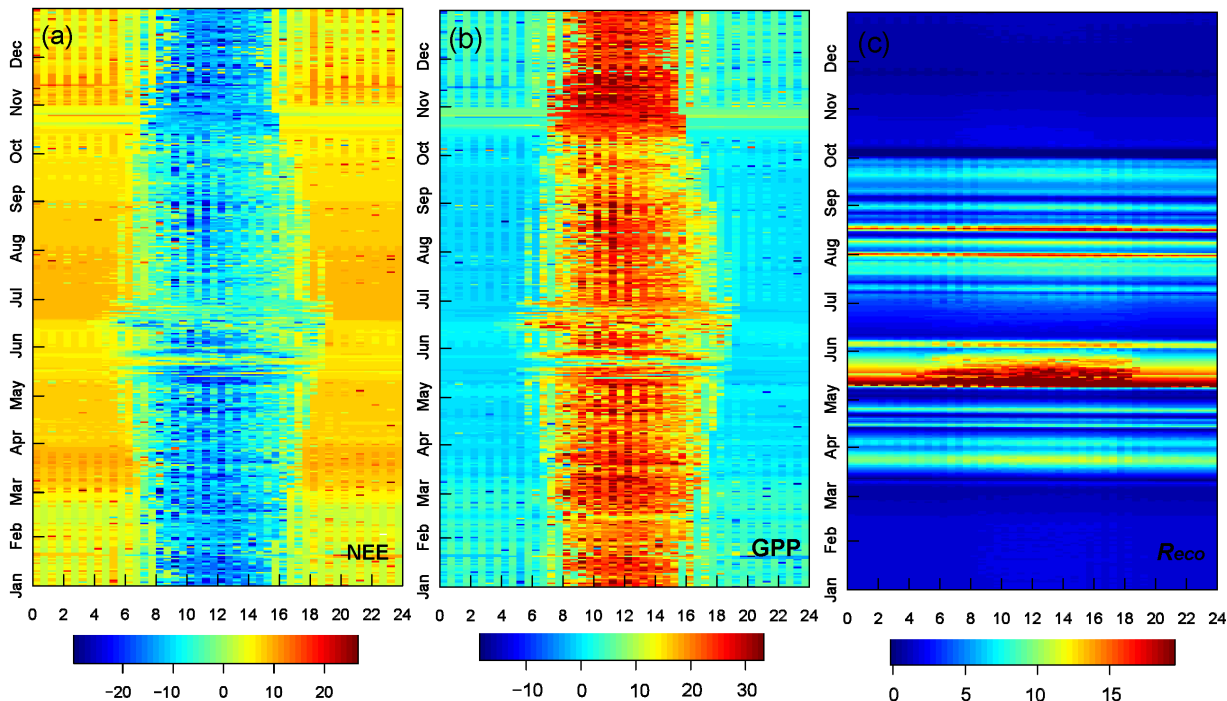
Figure 9. Seasonal changes on the fingerprints calculated by the REddyProc system in μmol m^{2}s^{-1} during the years 2005-2008: (a) NEE; (b) GPP; and (c) R_{eco} Daytime. The axis-x shows time (24h), UTC -4.

3.7 BBOA effects on the biophysical variables and NEE

These results are important as a large part of the Amazon area is frequently impacted by the presence of aerosols in small amounts (low AOD), similar to those observed in the north of the Amazon basin, in Manaus-AM. In regions with high rates of deforestation and biomass burning, however, increases in CO_2 absorption are significant and can have major impacts on the carbon budget of the Amazon forest. Over dense forest ecosystems of central Amazon, CO_2 absorption peaks are often observed at higher and narrower intervals of f (1.1 to 0.80), especially for dense forest ecosystems (Gu et al., 1999; Yamasoe et al., 2006; Oliveira et al., 2007; Doughty et al., 2010). This is different from grasslands and temperate forests, where the maximum net CO_2 uptake is generally found in the range f between 1.0-0.5 (Gu et al., 1999; Niyogi et al., 2004; Jing et al., 2010; Zhang et al., 2010).

The mechanisms to explain the variation in %NEE with the irradiance f are complex and influenced by the dynamics of the Planetary Boundary Layer (PBL) throughout the day, including transport of regionally transported and locally emitted burning emissions. For the semideciduous forests studied here, an accumulation of aerosols from fires during the night hours (19h to 06h, LT) maybe associated with greater stability in the PBL during the fire season (lower values in wind speed, reduction in convection and boundary layer narrowing). These factors can increase the concentration of aerosols (AOD$_a$) during the night,

with important effects on the CO_2 absorption capacity ($\%NEE$) observed in the early daytime hours (SZA values between 50-75°.

Future studies may elucidate the dynamic effects of PBL on the photosynthetic capacity of forests in the Amazon Basin, like studies carried out in other forests around the world, e.g., in Utah, USA, Helliker and Ehleringer (2000), UK, Yakir (2003), and Beijing, China, Wang et al. (2021, 2022). Field experiments focused on the vertical distribution of $PAR(D)_F$ throughout the canopy will improve the current understanding of the individual effects of aerosols and clouds on the forest microclimate (LC_T and VPD) on $\%NEE$.

Figure 10 shows significant interference of aerosols on environmental variables that consequently affect the photosynthetic dynamics of plants. The attenuating effect of incident solar irradiance due to the presence of aerosols triggers statistically significant reductions in LC_T, T_{air} and VPD near the forest canopy (Fig. 10). However, we noticed that T_{air} is wider than LC_T (Figs. 10b and 10a), which suggests that the LC_T fails to capture the realistic variability. To verify and evaluate the consistency of the LC_T model (Equation 9), calibrated to the Central Amazon conditions (mentioned in the subsubsection 2.3.7), a second method (LC_{Ts}), based on the Stefan-Boltzmann equation (Doughty et al., 2010; Cirino et al., 2014) was tested (see Equation S1, Figs. S9 and S10, supplementary material). We observed that T_{air} is systematically smaller throughout the day (Figs. S9b and S9a), results obtained from the same data points shown in Figures 10a and 10b. On average, the amplitude between LC_T and T_{air} is equal to 2.2 ($\pm$ 2.1) °C (Fig. S9c), and the leaf canopy is warmer than the air between 7-17h (LT), as expected. The leaf canopy was warmer than T_{air} during the day. However, the standard deviation (std) of LC_{Ts} is significantly higher. The amplitude between LC_{Ts} and T_{air} is about 1.7 $\pm$ 11.1 °C (Figs. S9a and S9b). LC_{Ts} appear to capture average hourly behavior but exhibit much greater hourly variability compared to T_{air} throughout the year. The LC_T results reveal an acceptable average hourly pattern for leaf canopy temperature, although the pattern is unrealistic compared to T_{air}. Due to the limitations of LC_T, it is worth mentioning that we are likely underestimating the uncertainties of aerosol effects on canopy temperature. However, the impact of aerosols in T_{air} also indicates an important cooling at the surface ($\sim$3-4 °C), with relevant effects on the canopy and functioning of the studied ecosystem.

Several mechanisms have been used to explain the increase in photosynthetic capacity by the canopy due to changes in the biophysical properties of the forest, among them, the general trend of decreasing temperatures (Koren et al., 2014; Bai et al., 2012) and VPD (Min, 2005; Yuan et al., 2019) under cloudy or smoky skies. The effect of this cooling, especially on the leaf canopy, can also exert considerable influence on the photosynthesis of the forest (Doughty et al., 2010; Vourlitis et al., 2011). Herein, the impact of aerosols produced, respectively, a cooling of 3 °C and 2.5 °C in the LC_T and T_{air} when f declined from 1.10 to 0.66 (Fig. 10a and Fig. 10b), ranges for the which NEE increase about of 3-7 μmol m^{-2}s^{-1} as discussed section before. These results are similar to the results found by Davidi et al. (2009) and Doughty et al. (2010) in the FLONA-Tapajos (Santarem-PA). However, the individual impacts of these effects depend on long-term and simultaneous measures of extrinsic factors (water stress, nutrient availability, solar radiation, aerosols, and cloud cover) and intrinsic aspects of the plant (forest type, leaf canopy structure, stomatal and roots structure), unavailable at the site and period studied. Moreover, the non-linear relationship between these factors makes it challenging to determine the physiological optimums for given biophysical variables, such as temperature and VPD.
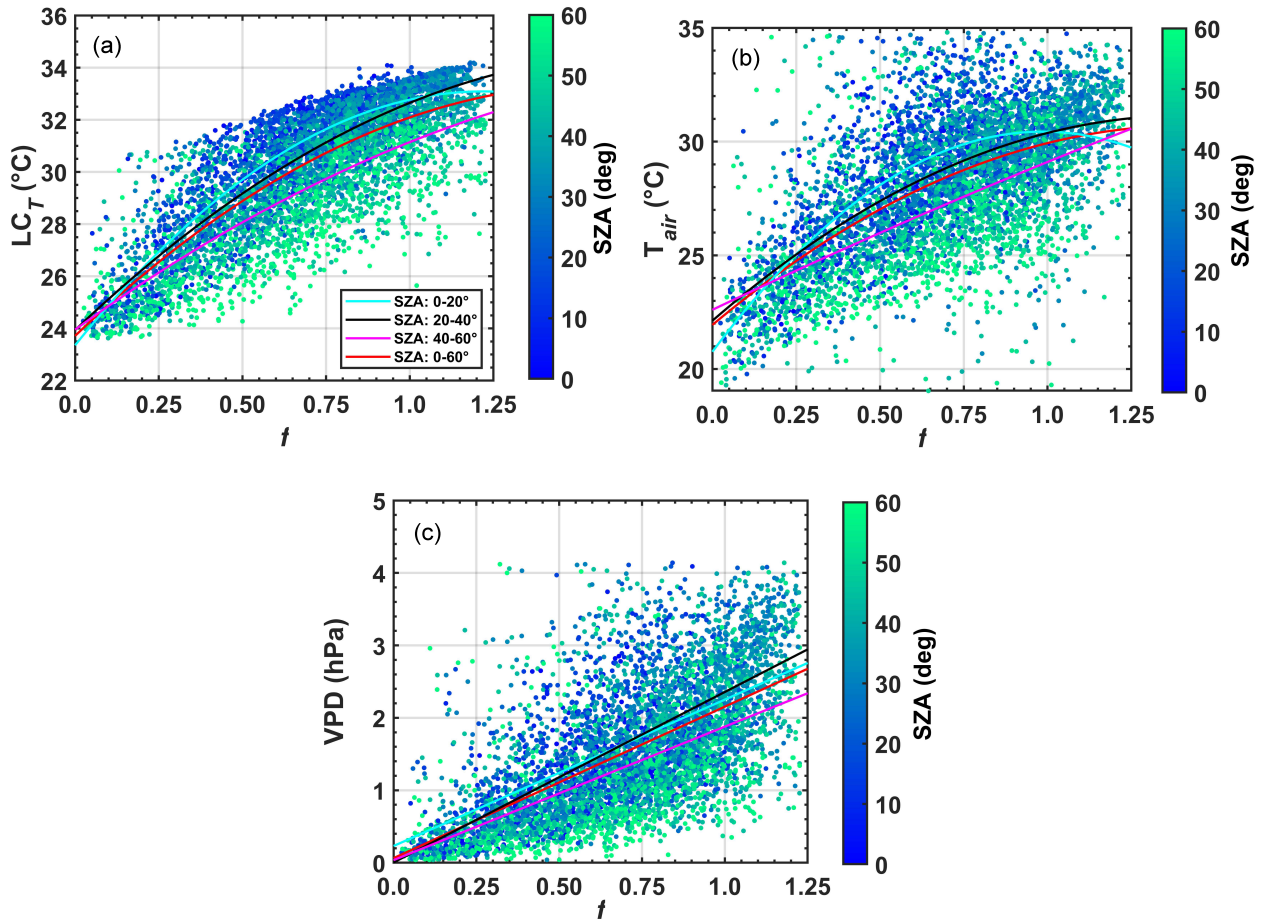
Figure 10. Correlation between the relative irradiance f versus LC_T (a), T_{air} (b) and VPD (c), values calculated for SZA between 0 and 60. The air temperature was measured at 42 m above the ground in the micrometeorological tower located in the municipality of Cláudia, 50 km from Sinop-MT, using the parameterization given in Tribuzy (2005), between 2003-2004.

The increase in relative humidity due to air cooling induced by clouds or aerosols can also influence photosynthesis (Freedman et al., 1998; Altaratz et al., 2008; Jing et al., 2010). In many forest locations, the reduction in f decreases VPD during the dry season. These reductions, strongly influenced by the cooling of the air, are also closely linked with the cooling of the forest canopy and the increase in the absorption capacity of CO_2 (%NEE) (Doughty et al., 2010), considering its physiological optimums (tipping points). For cloudy or polluted sky conditions, generally decreasing VPD behavior can influence stomata opening and intensify photosynthesis (Jing et al., 2010). Here, we observed a reduction of 2-3 hPa attributed to the decrease of around 3-4 (°C) in the air temperature, which agrees up to ∼40% reduction in f from which NEE is critically reduced. Furthermore, It is still possible that an enhancement in the NEE is related to an increase in transpiration rates, providing cooling in the air, i.e., positive feedback between AOD, NEE, and RU_{air} (Caioni et al., 2020).

580 Unlike what was found here, the forests of central Amazonia, in Manaus-AM (K34), FLONA-Tapajos (K83), Santarem-PA, and Ji-Parana (RO) seem to be less tolerant to the attenuation of sunlight-induced by clouds and aerosols. In our forest, the distribution of f is close to 0.66 for $AOD_a \gg 0.10$ Table 5. This value is 15-20% lower than values found in central Amazonia when the NEE reaches maximum negative values during the burning season ($f \sim 0.80$). This is the threshold value at which maximum carbon absorption is observed due to aerosol load in the JBR in the Ji-Parana JBR (south of the Amazon basin)

585 as well as in the Cuieiras reserve at K34, in Manaus-AM. These comparisons are relevant because higher (lower) amounts of aerosols and clouds in the Amazon region can cause certain types of forests to absorb even higher (lower) amounts of carbon throughout the day (Gu et al., 1999; Cirino et al., 2014). The $\%NEE$ frequency distribution patterns and their impacts on photosynthesis remain unknown for many other forest types in the Amazon and around the world. The results reported here are also consistent with calculations by Gu et al. (1999) for temperate forests in Canada, where negative maximums in NEE

590 flux occur for ranges f between 0.55–0.60.

The interannual variability of the relationship between the observed AOD_a, fire counts, and NEE could not be analyzed, mainly due to the lack of a long-time series of NEE flux data in the region. In the central Amazon, significant variability was observed from year to year. Higher $\%NEE$ were often found on days with high fire counts. However, water stress and nutrient availability also play an essential role in the carbon uptake capacity (Gatti et al., 2014; Hofhansl et al., 2016; Gatti

595 et al., 2021; Malhi et al., 2021). Joint modifications in these variables make it extremely difficult to quantify the individual effects of aerosols and clouds on the NEE. Field experiments taking measurements of all these aspects will yield studies with more robust and comprehensive conclusions on the ecosystem responses of Amazonian forests to external environmental disturbances such as fires.

4 Conclusions

600 The aerosol optical depth derived from the AERONET system proved to be a key variable in the elaboration of the clear sky solar irradiance model used to determine the relative irradiance f. The conceived model can be directed to other regions of the Amazon as long as they are within the same latitude range, where there are no SW_i measurements. The parameter f, allowed us to satisfactorily evaluate the radiative effects of aerosols from fires on the net absorption of carbon (NEE) by the studied semideciduous forest ecosystem. The radiative impacts on PAR_i and $PAR(D)$ allowed us to evaluate the impacts on the

605 canopy light use efficiency (LUE), which increased by $\sim$ 1-3% under polluted conditions (AOD_a). The changes in incident solar radiation and CO_2 flux (NEE) could be attributed to the combined effects of aerosols emitted locally, regionally, or transported from more distant regions, considering the applied methods.

In the studied semideciduous forest ecosystem, the (NEE) increased from 20-70% when the optical depth varied from 0.1 to 5.0 (on average). This effect was attributed to an average reduction of up to 40% in the amount of total PAR radiation, and also

610 to an increase of up to 50% in the diffuse fraction of radiation ($PAR(D)_F$). This increase in CO_2 absorption capacity by the ecosystem is closely linked to the floristic composition of the understory and certain types of forest species adapted to low light conditions, which consists of more efficient vegetation in capturing diffused light during the photosynthesis process. The results

show higher photosynthetic efficiency under smoky sky conditions; loaded with particles scattering solar radiation due to fires, but also reveal the maximum limit in the PAR radiation cuts required for the photosynthesis process. Relative irradiances f less than 0.66, on average, indicate the critical point at which forest photosynthetic rates undergo drastic reductions. Relative irradiance values $f \sim$ of 0.22 indicate 100% interruption in the photosynthetic process.

Due to the increase in the concentration of aerosol particles from fires in the region, statistically, significant changes were also observed in meteorological (biophysical) variables such as leaf canopy temperature and VPD. Scientific findings reveal a strong influence of fire aerosols on these variables, with potentially important effects on photosynthesis and carbon absorption. The 3 and 5 °C reductions in leaf canopy and air temperature are strongly associated with a 40% reduction in f and a $\sim$ 2.0 hPa reduction in VPD values which induce opening stomata and contribute to the observed increase of 20-70% in the CO_2 absorption capacity of the forest (%NEE). The individual influences or contributions of the VPD, T_{air} and LC_T to the ecosystem's net balance of CO_2, however, could not be directly quantified in this research. Indirect correlations, however, reveal statistically significant effects between the mentioned biophysical variables and the observed changes in the NEE flux during the exposure of forests to fire and high values of AOD_a (greater than 1.25, on average). Studies focused on the impacts of fires on the flux of water to the atmosphere deserve attention and can help to understand the role of forests in maintaining rainfall and its effects on the hydrological cycle (studies not yet carried out for most biomes in the Amazon).

4.1 Suggestions for future work

A more comprehensive regional study of the effects mentioned here, based on other vegetation types and biomes, using vegetation maps, remote sensing estimates, meteorological data, and numerical modeling, will help to better understand how the climate and ecosystem function in the Amazon are affected by natural and anthropic environmental. The reductions in the NEE flux and, therefore, the reduction of the photosynthetic capacity of the plants due to the excessive increase in the concentration of BBOA aerosols and drastic reductions in the fluxes of solar radiation ($f \leq 0.22$) due to the fires in the region, constitutes an effect of notable relevance for carbon cycling in semideciduous forest environments in the Amazon and, therefore, an important contribution to a better understanding of this cycle in the region. Future work would also involve estimating the global-scale significance of aerosol load on Photosynthetically Active Radiation (PAR) and, consequently, on Net Ecosystem Exchange (NEE) fluxes. In addition to the potential use of numerical modeling, promising approaches in this direction include research on remotely sensed solar-induced chlorophyll fluorescence (SIF) (Meroni et al. 2009). SIF has been increasingly utilized as a novel proxy for vegetation productivity. Comparing SIF with remotely sensed PAR_i and $PAR(D)$ (e.g., Rui et al. (2022); Zhang et al. (2023)) enables an observational-based global-scale comparison of the effects observed in this study and, potentially, the estimation of the impact of aerosol load in general, and biomass burning in particular, on the photosynthetic capacity of plants.

Data availability. This section provides free access to data repositories that support the conclusions. We provide the data from this survey available through the Mendeley Data platform (https://data.mendeley.com), where we will make upgrades and possible corrections. Citation: Cirino, Glauber; Vourlitis, George; Silva, Simone; Palácios, Rafael (2022), "Brazil-FluxMet-Stf", Mendeley Data, v2 DOI: 10.17632/m5h5fw872g.2. Secondary data is already in the public domain. We have listed the links to these data in the Supporting Information (Table S5)

Author contributions. Conceptualization and Methodology, S.R., G.C. and G.V.; Software, S.R., G.C., G.V. and R.P; Validation, G.V., G.C., R.P. and S.R.; Formal Analysis, The authors contributed equally to this work; Investigation, S.R., G.C., D.M., A.P., SC.L,B.I. and G.V.; Resources, G.V. and G.C.; Data Curation, G.V., J.N., G.C., R.P., and S.R.; Writing-original Draft Preparation, S.R. and G.C.; Writing-review and Editing, G.C., S.R., G.V., D.M., A.P., MI.V. and SC.L.; All authors have read and agreed to the published version of the manuscript.

Competing interests. No potential conflict of interest was reported by the authors.

Acknowledgements. We want to thank the Coordination for the Improvement of Higher Education Personnel (CAPES), the National Science Foundation, the National Council for Scientific and Technological Development (CNPq), the Mato Grosso State Research Support Foundation (FAPEMAT), the State University of California, San Marcos (CSUSM), to the Federal University of Mato Grosso (UFMT). Additional funding was provided by CNPq Universal, project 422894/2021-4, and by the Fundação de Amparo à Pesquisa do Estado do Pará (FAPESPA), grant 2022/45107. To PROPESP/UFPA, for the financial support to students. Special thanks to Dimensions Sciences Bridging Gaps with Scholarships (DS BRIDGES) - Amazon Task Force for providing social and financial support for the research of countless students in vulnerable situations. Our special thanks to Professor Dr. José de Souza Nogueira *(in memoriam)* who worked with other collaborators to generate and obtain micrometeorological data from the measuring tower used in this research.

References

Ackerly, D. D., Wayt Thomas, W., Cid Ferreira, C. A., and PIRANI Ackerly, R.: THE FOREST-CERRADO TRANSITION ZONE IN SOUTHERN AMAZONIA: RESULTS OF THE 1985 PROJETO FLORA AMAZONICA EXPEDITION TO MATO GROSSO, Brittonia, 41, 113–128, 1989.

Adachi, K., Oshima, N., Gong, Z., de Sá, S., Bateman, A. P., Martin, S. T., de Brito, J. F., Artaxo, P., Cirino, G. G., Sedlacek III, A. J., and Buseck, P. R.: Mixing states of Amazon basin aerosol particles transported over long distances using transmission electron microscopy, Atmospheric Chemistry and Physics, 20, 11 923–11 939, https://doi.org/10.5194/acp-20-11923-2020, 2020.

Alencar, A. A. C., Arruda, V. L. S., Silva, W. V. d., Conciani, D. E., Costa, D. P., Crusco, N., Duverger, S. G., Ferreira, N. C., Franca-Rocha, W., Hasenack, H., Martenexen, L. F. M., Piontekowski, V. J., Ribeiro, N. V., Rosa, E. R., Rosa, M. R., dos Santos, S. M. B., Shimbo, J. Z., and Vélez-Martin, E.: Long-Term Landsat-Based Monthly Burned Area Dataset for the Brazilian Biomes Using Deep Learning, Remote Sensing, 14, https://doi.org/10.3390/rs14112510, 2022.

Alencar A.; Nepstad D.; MacGrath D.; Moutinho, P.: Desmatamento na Amazônia: Indo além da emergência crônica, Tech. rep., IPAM, 2004.

Altaratz, O., Koren, I., and Reisin, T.: Humidity impact on the aerosol effect in warm cumulus clouds, Geophysical Research Letters, 35, 1–5, https://doi.org/10.1029/2008GL034178, 2008.

Anderegg, W. R., Trugman, A. T., Badgley, G., Konings, A. G., and Shaw, J.: Divergent forest sensitivity to repeated extreme droughts, Nature Climate Change, 10, 1091–1095, https://doi.org/10.1038/s41558-020-00919-1, 2020.

Aragão, L. E., Anderson, L. O., Fonseca, M. G., Rosan, T. M., Vedovato, L. B., Wagner, F. H., Silva, C. V., Silva Junior, C. H., Arai, E., Aguiar, A. P., Barlow, J., Berenguer, E., Deeter, M. N., Domingues, L. G., Gatti, L., Gloor, M., Malhi, Y., Marengo, J. A., Miller, J. B., Phillips, O. L., and Saatchi, S.: 21st Century drought-related fires counteract the decline of Amazon deforestation carbon emissions, Nature Communications, 9, 1–12, https://doi.org/10.1038/s41467-017-02771-y, 2018.

Araújo, A. C., Dolman, A. J., Waterloo, M. J., Gash, J. H., Kruijt, B., Zanchi, F. B., de Lange, J. M., Stoevelaar, R., Manzi, A. O., Nobre, A. D., Lootens, R. N., and Backer, J.: The spatial variability of CO2 storage and the interpretation of eddy covariance fluxes in central Amazonia, Agricultural and Forest Meteorology, 150, 226–237, https://doi.org/10.1016/j.agrformet.2009.11.005, 2010.

Artaxo, P., Rizzo, L. V., Brito, J. F., Barbosa, H. M., Arana, A., Sena, E. T., Cirino, G. G., Bastos, W., Martin, S. T., and Andreae, M. O.: Atmospheric aerosols in Amazonia and land use change: From natural biogenic to biomass burning conditions, Faraday Discussions, 165, 203–235, https://doi.org/10.1039/c3fd00052d, 2013.

Artaxo, P., Hansson, H.-C., Andreae, M. O., Bäck, J., Alves, E. G., Barbosa, H. M. J., Bender, F., Bourtsoukidis, E., Carbone, S., Chi, J., Decesari, S., Després, V. R., Ditas, F., Ezhova, E., Fuzzi, S., Hasselquist, N. J., Heintzenberg, J., Holanda, B. A., Guenther, A., Hakola, H., Heikkinen, L., Kerminen, V.-M., Kontkanen, J., Krejci, R., Kulmala, M., Lavric, J. V., de Leeuw, G., Lehtipalo, K., Machado, L. A. T., McFiggans, G., Franco, M. A. M., Meller, B. B., Morais, F. G., Mohr, C., Morgan, W., Nilsson, M. B., Peichl, M., Petäjä, T., Praß, M., Pöhlker, C., Pöhlker, M. L., Pöschl, U., Von Randow, C., Riipinen, I., Rinne, J., Rizzo, L. V., Rosenfeld, D., Silva Dias, M. A. F., Sogacheva, L., Stier, P., Swietlicki, E., Sörgel, M., Tunved, P., Virkkula, A., Wang, J., Weber, B., Yáñez-Serrano, A. M., Zieger, P., Mikhailov, E., Smith, J. N., and Kesselmeier, J.: Tropical and Boreal Forest – Atmosphere Interactions: A Review, Tellus B: Chemical and Physical Meteorology, https://doi.org/10.16993/tellusb.34, 2022.

Aubinet, M.: Eddy Covariance, https://doi.org/10.1007/978-94-007-2351-1, 2012.

Aubinet, M., Chermanne, B., Vandenhaute, M., Longdoz, B., Yernaux, M., and Laitat, E.: Long term carbon dioxide exchange above a mixed forest in the Belgian Ardennes, Agricultural and Forest Meteorology, 108, 293–315, https://doi.org/10.1016/S0168-1923(01)00244-1, 2001.

Avitabile, V., Herold, M., Heuvelink, G. B., Lewis, S. L., Phillips, O. L., Asner, G. P., Armston, J., Ashton, P. S., Banin, L., Bayol, N., Berry, N. J., Boeckx, P., de Jong, B. H., Devries, B., Girardin, C. A., Kearsley, E., Lindsell, J. A., Lopez-Gonzalez, G., Lucas, R., Malhi, Y., Morel, A., Mitchard, E. T., Nagy, L., Qie, L., Quinones, M. J., Ryan, C. M., Ferry, S. J., Sunderland, T., Laurin, G. V., Gatti, R. C., Valentini, R., Verbeeck, H., Wijaya, A., and Willcock, S.: An integrated pan-tropical biomass map using multiple reference datasets, Global Change Biology, 22, 1406–1420, https://doi.org/10.1111/gcb.13139, 2016.

Bai, Y., Wang, J., Zhang, B., Zhang, Z., and Liang, J.: Comparing the impact of cloudiness on carbon dioxide exchange in a grassland and a maize cropland in northwestern China, Ecological Research, 27, 615–623, https://doi.org/10.1007/s11284-012-0930-z, 2012.

Balch, J. K., Brando, P. M., Nepstad, D. C., Coe, M. T., Silvério, D., Massad, T. J., Davidson, E. A., Lefebvre, P., Oliveira-Santos, C., Rocha, W., Cury, R. T., Parsons, A., and Carvalho, K. S.: The Susceptibility of Southeastern Amazon Forests to Fire: Insights from a Large-Scale Burn Experiment, BioScience, 65, 893–905, https://doi.org/10.1093/biosci/biv106, 2015.

Barbosa, F. R. G. M., Duarte, V. N., Staduto, J. A. R., and Kreter, A. C.: Land-Use Dynamics for Agricultural and Livestock in Central-West Brazil and its Reflects on the Agricultural Frontier Expansion, Cleaner and Circular Bioeconomy, 4, 100 033, https://doi.org/10.1016/j.clcb.2022.100033, 2023.

Beer, C., Reichstein, M., Tomelleri, E., Ciais, P., Jung, M., Carvalhais, N., Rödenbeck, C., Arain, M. A., Baldocchi, D., Bonan, G. B., Bondeau, A., Cescatti, A., Lasslop, G., Lindroth, A., Lomas, M., Luyssaert, S., Margolis, H., Oleson, K. W., Roupsard, O., Veenendaal, E., Viovy, N., Williams, C., Woodward, F. I., and Papale, D.: Terrestrial gross carbon dioxide uptake: Global distribution and covariation with climate, Science, 329, 834–838, https://doi.org/10.1126/science.1184984, 2010.

Bian, H., Lee, E., Koster, R. D., Barahona, D., Chin, M., Colarco, P. R., Darmenov, A., Mahanama, S., Manyin, M., Norris, P., Shilling, J., Yu, H., and Zeng, F.: The response of the Amazon ecosystem to the photosynthetically active radiation fields: Integrating impacts of biomass burning aerosol and clouds in the NASA GEOS Earth system model, Atmospheric Chemistry and Physics, 21, 14 177–14 197, https://doi.org/10.5194/acp-21-14177-2021, 2021.

Bird, R. E., Hulstrom, R.: A Simplifield Clear Sky Model for Direct and Diffuse Insolation on Horizontal Surfaces, 1981.

Booth, B. B., Jones, C. D., Collins, M., Totterdell, I. J., Cox, P. M., Sitch, S., Huntingford, C., Betts, R. A., Harris, G. R., and Lloyd, J.: High sensitivity of future global warming to land carbon cycle processes, Environmental Research Letters, 7, https://doi.org/10.1088/1748-9326/7/2/024002, 2012.

Brando, P. M., Balch, J. K., Nepstad, D. C., Morton, D. C., Putz, F. E., Coe, M. T., Silvério, D., Macedo, M. N., Davidson, E. A., Nóbrega, C. C., Alencar, A., and Soares-Filho, B. S.: Abrupt increases in Amazonian tree mortality due to drought-fire interactions, Proceedings of the National Academy of Sciences of the United States of America, 111, 6347–6352, https://doi.org/10.1073/pnas.1305499111, 2014.

Brando, P. M., Silvério, D., Maracahipes-Santos, L., Oliveira-Santos, C., Levick, S. R., Coe, M. T., Migliavacca, M., Balch, J. K., Macedo, M. N., Nepstad, D. C., Maracahipes, L., Davidson, E., Asner, G., Kolle, O., and Trumbore, S.: Prolonged tropical forest degradation due to compounding disturbances: Implications for CO2 and H2O fluxes, Global Change Biology, 25, 2855–2868, https://doi.org/10.1111/gcb.14659, 2019.

Brienen, R. J., Phillips, O. L., Feldpausch, T. R., Gloor, E., Baker, T. R., Lloyd, J., Lopez-Gonzalez, G., Monteagudo-Mendoza, A., Malhi, Y., Lewis, S. L., Vásquez Martinez, R., Alexiades, M., Álvarez Dávila, E., Alvarez-Loayza, P., Andrade, A., Aragaõ, L. E., Araujo-Murakami, A., Arets, E. J., Arroyo, L., Aymard C., G. A., Bánki, O. S., Baraloto, C., Barroso, J., Bonal, D., Boot, R. G., Camargo, J. L., Castilho,

C. V., Chama, V., Chao, K. J., Chave, J., Comiskey, J. A., Cornejo Valverde, F., Da Costa, L., De Oliveira, E. A., Di Fiore, A., Erwin, T. L., Fauset, S., Forsthofer, M., Galbraith, D. R., Grahame, E. S., Groot, N., Hérault, B., Higuchi, N., Honorio Coronado, E. N., Keeling, H., Killeen, T. J., Laurance, W. F., Laurance, S., Licona, J., Magnussen, W. E., Marimon, B. S., Marimon-Junior, B. H., Mendoza, C., Neill, D. A., Nogueira, E. M., Núñez, P., Pallqui Camacho, N. C., Parada, A., Pardo-Molina, G., Peacock, J., Penã-Claros, M., Pickavance, G. C., Pitman, N. C., Poorter, L., Prieto, A., Quesada, C. A., Ramírez, F., Ramírez-Angulo, H., Restrepo, Z., Roopsind, A., Rudas, A., Salomão, R. P., Schwarz, M., Silva, N., Silva-Espejo, J. E., Silveira, M., Stropp, J., Talbot, J., Ter Steege, H., Teran-Aguilar, J., Terborgh, J., Thomas-Caesar, R., Toledo, M., Torello-Raventos, M., Umetsu, R. K., Van Der Heijden, G. M., Van Der Hout, P., Guimarães Vieira, I. C., Vieira, S. A., Vilanova, E., Vos, V. A., and Zagt, R. J.: Long-term decline of the Amazon carbon sink, Nature, 519, 344–348, https://doi.org/10.1038/nature14283, 2015.

Burba, G.: Eddy Covariance Method for Scientific, Industrial, Agricultural and Regulatory Applications: A Field Book on Measuring Ecosystem Gas Exchange and Areal Emission Rates, https://doi.org/10.13140/RG.2.1.4247.8561, 2013.

Caioni, C., Silvério, D. V., Macedo, M. N., Coe, M. T., and Brando, P. M.: Droughts amplify differences between the energy balance components of Amazon forests and croplands, Remote Sensing, 12, https://doi.org/10.3390/rs12030525, 2020.

Carswell, F. E., Costa, A. L., Palheta, M., Malhi, Y., Meir, P., Costa, J. d. P. R., Ruivo, M. d. L., Leal, L. d. S. M., Costa, J. M. N., Clement, R. J., and Grace, J.: Seasonality in CO2 and H2O flux at an eastern Amazonian rain forest, Journal of Geophysical Research: Atmospheres, 107, LBA 43–1–LBA 43–16, https://doi.org/https://doi.org/10.1029/2000JD000284, 2002.

Cirino, G., Brito, J., Barbosa, H. M., Rizzo, L. V., Tunved, P., de Sá, S. S., Jimenez, J. L., Palm, B. B., Carbone, S., Lavric, J. V., Souza, R. A., Wolff, S., Walter, D., Tota, J., Oliveira, M. B., Martin, S. T., and Artaxo, P.: Observations of Manaus urban plume evolution and interaction with biogenic emissions in GoAmazon 2014/5, Atmospheric Environment, 191, 513–524, https://doi.org/10.1016/j.atmosenv.2018.08.031, 2018.

Cirino, G. G., Souza, R. A., Adams, D. K., and Artaxo, P.: The effect of atmospheric aerosol particles and clouds on net ecosystem exchange in the Amazon, Atmospheric Chemistry and Physics, 14, 6523–6543, https://doi.org/10.5194/acp-14-6523-2014, 2014.

Corripio, J. G.: Vectorial algebra algorithms for calculating terrain parameters from DEMs and solar radiation modelling in mountainous terrain, 17, 1–23, https://doi.org/10.1080/13658810210157796, 2003.

Corwin, K. A., Corr, C. A., Burkhardt, J., and Fischer, E. V.: Smoke-Driven Changes in Photosynthetically Active Radiation During the U.S. Agricultural Growing Season, Journal of Geophysical Research: Atmospheres, 127, e2022JD037 446, https://doi.org/https://doi.org/10.1029/2022JD037446, e2022JD037446 2022JD037446, 2022.

Davidi, A., Koren, I., and Remer, L.: Direct measurements of the effect of biomass burning over the Amazon on the atmospheric temperature profile, Atmospheric Chemistry and Physics, 9, 8211–8221, https://doi.org/10.5194/acp-9-8211-2009, 2009.

Davison, C. W., Rahbek, C., and Morueta-Holme, N.: Land-use change and biodiversity: Challenges for assembling evidence on the greatest threat to nature, https://doi.org/10.1111/gcb.15846, 2021.

de Magalhães, N., Evangelista, H., Condom, T., Rabatel, A., and Ginot, P.: Amazonian Biomass Burning Enhances Tropical Andean Glaciers Melting, Scientific Reports, 9, 1–12, https://doi.org/10.1038/s41598-019-53284-1, 2019.

de Sá, S. S., Rizzo, L. V., Palm, B. B., Campuzano-Jost, P., Day, D. A., Yee, L. D., Wernis, R., Isaacman-VanWertz, G., Brito, J., Carbone, S., Liu, Y. J., Sedlacek, A., Springston, S., Goldstein, A. H., Barbosa, H. M. J., Alexander, M. L., Artaxo, P., Jimenez, J. L., and Martin, S. T.: Contributions of biomass-burning, urban, and biogenic emissions to the concentrations and light-absorbing properties of particulate matter in central Amazonia during the dry season, Atmospheric Chemistry and Physics, 19, 7973–8001, https://doi.org/10.5194/acp-19-7973-2019, 2019.

Doughty, C. E., Flanner, M. G., and Goulden, M. L.: Effect of smoke on subcanopy shaded light, canopy temperature, and carbon dioxide uptake in an Amazon rainforest, Global Biogeochemical Cycles, 24, 1–10, https://doi.org/10.1029/2009GB003670, 2010.

Doughty, C. E., Metcalfe, D. B., Girardin, C. A., Amézquita, F. F., Cabrera, D. G., Huasco, W. H., Silva-Espejo, J. E., Araujo-Murakami, A., Da Costa, M. C., Rocha, W., Feldpausch, T. R., Mendoza, A. L., Da Costa, A. C., Meir, P., Phillips, O. L., and Malhi, Y.: Drought impact on forest carbon dynamics and fluxes in Amazonia, Nature, 519, 78–82, https://doi.org/10.1038/nature14213, 2015.

Drugé, T., Nabat, P., Mallet, M., Michou, M., Rémy, S., and Dubovik, O.: Modeling radiative and climatic effects of brown carbon aerosols with the ARPEGE-Climat global climate model, Atmospheric Chemistry and Physics, 22, 12 167–12 205, https://doi.org/10.5194/acp-22-12167-2022, 2022.

Duchon, C. E. and O'Malley, M. S.: Estimating Cloud Type from Pyranometer Observations, Journal of Applied Meteorology, 38, 132 – 141, https://doi.org/https://doi.org/10.1175/1520-0450(1999)038<0132:ECTFPO>2.0.CO;2, 1999.

Durand, M., Murchie, E. H., Lindfors, A. V., Urban, O., Aphalo, P. J., and Robson, T. M.: Diffuse solar radiation and canopy photosynthesis in a changing environment, Agricultural and Forest Meteorology, 311, https://doi.org/10.1016/j.agrformet.2021.108684, 2021.

Finnigan, J.: The storage term in eddy flux calculations, Agricultural and Forest Meteorology, 136, 108–113, https://doi.org/10.1016/j.agrformet.2004.12.010, 2006.

Freedman, J., Fitzjarrald, D., Moore, K., and Sakai, R.: Boundary layer cloud climatology and enhanced forest-atmosphere exchange, in: Preprints of 23rd Conference on Agricultural and Forest Meteorology, pp. 41–44, 1998.

Fu, Z., Gerken, T., Bromley, G., Araújo, A., Bonal, D., Burban, B., Ficklin, D., Fuentes, J. D., Goulden, M., Hirano, T., Kosugi, Y., Liddell, M., Nicolini, G., Niu, S., Roupsard, O., Stefani, P., Mi, C., Tofte, Z., Xiao, J., Valentini, R., Wolf, S., and Stoy, P. C.: The surface-atmosphere exchange of carbon dioxide in tropical rainforests: Sensitivity to environmental drivers and flux measurement methodology, Agricultural and Forest Meteorology, 263, 292–307, https://doi.org/10.1016/j.agrformet.2018.09.001, 2018.

Fuentes, J. D., Chamecki, M., Dos Santos, R. M. N., Von Randow, C., Stoy, P. C., Katul, G., Fitzjarrald, D., Manzi, A., Gerken, T., Trowbridge, A., Freire, L. S., Ruiz-Plancarte, J., Maia, J. M. F., Tóta, J., Dias, N., Fisch, G., Schumacher, C., Acevedo, O., Mercer, J. R., and Yañez-Serrano, A. M.: Linking meteorology, turbulence, and air chemistry in the amazon rain forest, Bulletin of the American Meteorological Society, 97, 2329–2342, https://doi.org/10.1175/BAMS-D-15-00152.1, 2016.

Gao, Y.: Atmospheric Aerosols Elevated Ecosystem Productivity of a Poplar Plantation in Beijing, 2 China, 2020.

Gates, D. M.: Biophysical Ecology, 1980.

Gatti, L. V., Gloor, M., Miller, J. B., Doughty, C. E., Malhi, Y., Domingues, L. G., Basso, L. S., Martinewski, A., Correia, C. S., Borges, V. F., Freitas, S., Braz, R., Anderson, L. O., Rocha, H., Grace, J., Phillips, O. L., and Lloyd, J.: Drought sensitivity of Amazonian carbon balance revealed by atmospheric measurements, Nature, 506, 76–80, https://doi.org/10.1038/nature12957, 2014.

Gatti, L. V., Basso, L. S., Miller, J. B., Gloor, M., Gatti Domingues, L., Cassol, H. L., Tejada, G., Aragão, L. E., Nobre, C., Peters, W., Marani, L., Arai, E., Sanches, A. H., Corrêa, S. M., Anderson, L., Von Randow, C., Correia, C. S., Crispim, S. P., and Neves, R. A.: Amazonia as a carbon source linked to deforestation and climate change, Nature, 595, 388–393, https://doi.org/10.1038/s41586-021-03629-6, 2021.

Grace, J., Malhi, Y., Lloyd, J., McIntyre, J., Miranda, A. C., Meir, P., and Miranda, H. S.: The use of eddy covariance to infer the net carbon dioxide uptake of Brazilian rain forest, Global Change Biology, 2, 209–217, https://doi.org/10.1111/j.1365-2486.1996.tb00073.x, 1996.

Green, J. K., Berry, J., Ciais, P., Zhang, Y., and Gentine, P.: Amazon rainforest photosynthesis increases in response to atmospheric dryness, Tech. rep., https://www.science.org, 2020.

Gu, L., Fuentes, J. D., Shugart, H. H., Staebler, R. M., and Black, T. A.: Responses of net ecosystem exchanges of carbon dioxide to changes in cloudiness: Results from two North American deciduous forests, Journal of Geophysical Research Atmospheres, 104, 31421–31434, https://doi.org/10.1029/1999JD901068, 1999.

Gu, L., Fuentes, J. D., Garstang, M., Silva, J. T. D., Heitz, R., Sigler, J., and Shugart, H. H.: Cloud modulation of surface solar irradiance at a pasture site in Southern Brazil, Agricultural and Forest Meteorology, 106, 117–129, https://doi.org/10.1016/S0168-1923(00)00209-4, 2001.

Gu, L., Baldocchi, D. D., Wofsy, S. C., Munger, J. W., Michalsky, J. J., Urbanski, S. P., and Boden, T. A.: Response of a Deciduous Forest to the Mount Pinatubo Eruption: Enhanced Photosynthesis, Science, 299, 2035–2038, https://doi.org/10.1126/science.1078366, 2003.

Helliker, B. R. and Ehleringer, J. R.: Establishing a grassland signature in veins: ^{18}O in the leaf water of C$_3$ and C$_4$ grasses, Proceedings of the National Academy of Sciences, 97, 7894–7898, https://doi.org/10.1073/pnas.97.14.7894, 2000.

Hofhansl, F., Andersen, K. M., Fleischer, K., Fuchslueger, L., Rammig, A., Schaap, K. J., Valverde-Barrantes, O. J., and Lapola, D. M.: Amazon forest ecosystem responses to elevated atmospheric Co2 and alterations in nutrient availability: Filling the gaps with model-experiment integration, Frontiers in Earth Science, 4, 1–9, https://doi.org/10.3389/feart.2016.00019, 2016.

Holanda, B. A., Franco, M. A., Walter, D., Artaxo, P., Carbone, S., Cheng, Y., Chowdhury, S., Ditas, F., Gysel-Beer, M., Klimach, T., Kremper, L. A., Krüger, O. O., Lavric, J. V., Lelieveld, J., Ma, C., Machado, L. A. T., Modini, R. L., Morais, F. G., Pozzer, A., Saturno, J., Su, H., Wendisch, M., Wolff, S., Pöhlker, M. L., Andreae, M. O., Pöschl, U., and Pöhlker, C.: African biomass burning affects aerosol cycling over the Amazon, Communications Earth & Environment, 4, 154, https://doi.org/10.1038/s43247-023-00795-5, 2023.

Holben, B. N., Eck, T. F., Slutsker, I., Tanré, D., Buis, J. P., Setzer, A., Vermote, E., Reagan, J. A., Kaufman, Y. J., Nakajima, T., Lavenu, F., Jankowiak, I., and Smirnov, A.: AERONET - A federated instrument network and data archive for aerosol characterization, Remote Sensing of Environment, 66, 1–16, https://doi.org/10.1016/S0034-4257(98)00031-5, 1998.

Hubau, W., Lewis, S. L., Phillips, O. L., Affum-Baffoe, K., Beeckman, H., Cuní-Sanchez, A., Daniels, A. K., Ewango, C. E., Fauset, S., Mukinzi, J. M., Sheil, D., Sonké, B., Sullivan, M. J., Sunderland, T. C., Taedoumg, H., Thomas, S. C., White, L. J., Abernethy, K. A., Adu-Bredu, S., Amani, C. A., Baker, T. R., Banin, L. F., Baya, F., Begne, S. K., Bennett, A. C., Benedet, F., Bitariho, R., Bocko, Y. E., Boeckx, P., Boundja, P., Brienen, R. J., Brncic, T., Chezeaux, E., Chuyong, G. B., Clark, C. J., Collins, M., Comiskey, J. A., Coomes, D. A., Dargie, G. C., de Haulleville, T., Kamdem, M. N. D., Doucet, J. L., Esquivel-Muelbert, A., Feldpausch, T. R., Fofanah, A., Foli, E. G., Gilpin, M., Gloor, E., Gonmadje, C., Gourlet-Fleury, S., Hall, J. S., Hamilton, A. C., Harris, D. J., Hart, T. B., Hockemba, M. B., Hladik, A., Ifo, S. A., Jeffery, K. J., Jucker, T., Yakusu, E. K., Kearsley, E., Kenfack, D., Koch, A., Leal, M. E., Levesley, A., Lindsell, J. A., Lisingo, J., Lopez-Gonzalez, G., Lovett, J. C., Makana, J. R., Malhi, Y., Marshall, A. R., Martin, J., Martin, E. H., Mbayu, F. M., Medjibe, V. P., Mihindou, V., Mitchard, E. T., Moore, S., Munishi, P. K., Bengone, N. N., Ojo, L., Ondo, F. E., Peh, K. S., Pickavance, G. C., Poulsen, A. D., Poulsen, J. R., Qie, L., Reitsma, J., Rovero, F., Swaine, M. D., Talbot, J., Taplin, J., Taylor, D. M., Thomas, D. W., Toirambe, B., Mukendi, J. T., Tuagben, D., Umunay, P. M., van der Heijden, G. M., Verbeeck, H., Vleminckx, J., Willcock, S., Wöll, H., Woods, J. T., and Zemagho, L.: Asynchronous carbon sink saturation in African and Amazonian tropical forests, Nature, 579, 80–87, https://doi.org/10.1038/s41586-020-2035-0, 2020.

Huntingford, C., Zelazowski, P., Galbraith, D., Mercado, L. M., Sitch, S., Fisher, R., Lomas, M., Walker, A. P., Jones, C. D., Booth, B. B., Malhi, Y., Hemming, D., Kay, G., Good, P., Lewis, S. L., Phillips, O. L., Atkin, O. K., Lloyd, J., Gloor, E., Zaragoza-Castells, J., Meir, P., Betts, R., Harris, P. P., Nobre, C., Marengo, J., and Cox, P. M.: Simulated resilience of tropical rainforests to CO2 -induced climate change, Nature Geoscience, 6, 268–273, https://doi.org/10.1038/ngeo1741, 2013.

Jing, X., Huang, J., Wang, G., Higuchi, K., Bi, J., Sun, Y., Yu, H., and Wang, T.: The effects of clouds and aerosols on net ecosystem CO_2 exchange over semi-arid Loess Plateau of Northwest China, Atmospheric Chemistry and Physics, 10, 8205–8218, https://doi.org/10.5194/acp-10-8205-2010, 2010.

Kanniah, K. D., Beringer, J., North, P., and Hutley, L.: Control of atmospheric particles on diffuse radiation and terrestrial plant productivity: A review, Progress in Physical Geography, 36, 209–237, https://doi.org/10.1177/0309133311434244, 2012.

Koren, I., Dagan, G., and Altaratz, O.: From aerosol-limited to invigoration of warm convective clouds, Science, 344, 1143–1146, https://doi.org/10.1126/science.1252595, 2014.

Levy, R. C., Mattoo, S., Munchak, L. A., Remer, L. A., Sayer, A. M., Patadia, F., and Hsu, N. C.: The Collection 6 MODIS aerosol products over land and ocean, Atmospheric Measurement Techniques, 6, 2989–3034, https://doi.org/10.5194/amt-6-2989-2013, 2013.

Lorenzi, H.: Arvores , brasileiras, São Paulo, 2000.

Lorenzi, H.: Arvores , brasileiras, Sao Paulo, 2002.

Malavelle, F. F., Haywood, J. M., Mercado, L. M., Folberth, G. A., Bellouin, N., Sitch, S., and Artaxo, P.: Studying the impact of biomass burning aerosol radiative and climate effects on the Amazon rainforest productivity with an Earth system model, Atmospheric Chemistry and Physics, 19, 1301–1326, https://doi.org/10.5194/acp-19-1301-2019, 2019.

Malhi, Y.: The productivity, metabolism and carbon cycle of tropical forest vegetation, Journal of Ecology, 100, 65–75, https://doi.org/10.1111/j.1365-2745.2011.01916.x, 2012.

Malhi, Y., Melack, J., Gatti, L. V., Ometto, J. P., Kesselmeier, J., Wolff, S., Aragão, L. E. O., Costa, M. H., Saleska, S. R., Pangala, S., Basso, L. S., Rizzo, L., de Araújo, A. C., Restrepo-Coupe, N., and Silva Junior, C. H. L.: Chapter 6: Biogeochemical Cycles in the Amazon, https://doi.org/10.55161/takr3454, 2021.

Martin, S. T., Andreae, M. O., Althausen, D., Artaxo, P., Baars, H., Borrmann, S., Chen, Q., Farmer, D. K., Guenther, A., Gunthe, S. S., Jimenez, J. L., Karl, T., Longo, K., Manzi, A., Müller, T., Pauliquevis, T., Petters, M. D., Prenni, A. J., Pöschl, U., Rizzo, L. V., Schneider, J., Smith, J. N., Swietlicki, E., Tota, J., Wang, J., Wiedensohler, A., and Zorn, S. R.: An overview of the Amazonian Aerosol Characterization Experiment 2008 (AMAZE-08), Atmospheric Chemistry and Physics, 10, 11 415–11 438, https://doi.org/10.5194/acp-10-11415-2010, 2010a.

Martin, S. T., Andreae, M. O., Artaxo, P., Baumgardner, D., Chen, Q., Goldstein, A. H., Guenther, A., Heald, C. L., Mayol-Bracero, O. L., McMurry, P. H., Pauliquevis, T., Pschl, U., Prather, K. A., Roberts, G. C., Saleska, S. R., Silva Dias, M. A., Spracklen, D. V., Swietlicki, E., and Trebs, I.: Sources and properties of Amazonian aerosol particles, Reviews of Geophysics, 48, https://doi.org/10.1029/2008RG000280, 2010b.

MATLAB: version 9.8.8.748 (R2013a), The MathWorks Inc., Natick, Massachusetts, 2013.

Mercado, L. M., Bellouin, N., Sitch, S., Boucher, O., Huntingford, C., Wild, M., and Cox, P. M.: Impact of changes in diffuse radiation on the global land carbon sink, Nature, 458, 1014–1017, https://doi.org/10.1038/nature07949, 2009.

Meyers, T. P. and Dale, R. F.: Predicting daily insolation with hourly cloud height and coverage., https://doi.org/10.1175/1520-0450(1983)022<0537:PDIWHC>2.0.CO;2, 1983.

Min, Q.: Impacts of aerosols and clouds on forest-atmosphere carbon exchange, Journal of Geophysical Research: Atmospheres, 110, https://doi.org/https://doi.org/10.1029/2004JD004858, 2005.

Montagnani, L., Grünwald, T., Kowalski, A., Mammarella, I., Merbold, L., Metzger, S., Sedlák, P., and Siebicke, L.: Estimating the storage term in eddy covariance measurements: The ICOS methodology, International Agrophysics, 32, 551–567, https://doi.org/10.1515/intag-2017-0037, 2018.

Moreira, D. S., Freitas, S. R., Bonatti, J. P., Mercado, L. M., É. Rosário, N. M., Longo, K. M., Miller, J. B., Gloor, M., and Gatti, L. V.:
Coupling between the JULES land-surface scheme and the CCATT-BRAMS atmospheric chemistry model (JULES-CCATT-BRAMS1.0):
Applications to numerical weather forecasting and the CO2 budget in South America, Geoscientific Model Development, 6, 1243–1259,
https://doi.org/10.5194/gmd-6-1243-2013, 2013.

Moreira, D. S., Longo, K. M., Freitas, S. R., Yamasoe, M. A., Mercado, L. M., Rosário, N. E., Gloor, E., Viana, R. S., Miller, J. B., Gatti,
L. V., Wiedemann, K. T., Domingues, L. K., and Correia, C. C.: Modeling the radiative effects of biomass burning aerosols on carbon
fluxes in the Amazon region, Atmospheric Chemistry and Physics, 17, 14 785–14 810, https://doi.org/10.5194/acp-17-14785-2017, 2017.

Morgan, W. T., Darbyshire, E., Spracklen, D. V., Artaxo, P., and Coe, H.: Non-deforestation drivers of fires are increasingly important sources
of aerosol and carbon dioxide emissions across Amazonia, Scientific Reports, 9, 1–15, https://doi.org/10.1038/s41598-019-53112-6, 2019.

Murphy, P. G. and Lugo, A. E.: Ecology of tropical dry forest., Annual review of ecology and systematics. Vol. 17, pp. 67–88,
https://doi.org/10.1146/annurev.es.17.110186.000435, 1986.

Nagy, L., Artaxo, P., and Forsberg, B. R.: Interactions Between Biosphere, Atmosphere, and Human Land Use in the Amazon Basin: An
Introduction, https://doi.org/10.1007/978-3-662-49902-3_1, 2016.

Nagy, R. C., Porder, S., Brando, P., Davidson, E. A., Figueira, A. M. e. S., Neill, C., Riskin, S., and Trumbore, S.: Soil Carbon Dy-
namics in Soybean Cropland and Forests in Mato Grosso, Brazil, Journal of Geophysical Research: Biogeosciences, 123, 18–31,
https://doi.org/https://doi.org/10.1002/2017JG004269, 2018.

Nepstad, D., McGrath, D., Stickler, C., Alencar, A., Azevedo, A., Swette, B., Bezerra, T., DiGiano, M., Shimada, J., Da Motta, R. S., Armijo,
E., Castello, L., Brando, P., Hansen, M. C., McGrath-Horn, M., Carvalho, O., and Hess, L.: Slowing Amazon deforestation through public
policy and interventions in beef and soy supply chains, Science, 344, 1118–1123, https://doi.org/10.1126/science.1248525, 2014.

Niyogi, D., Chang, H. I., Saxena, V. K., Holt, T., Alapaty, K., Booker, F., Chen, F., Davis, K. J., Holben, B., Matsui, T., Meyers, T., Oechel,
W. C., Pielke, R. A., Wells, R., Wilson, K., and Xue, Y.: Direct observations of the effects of aerosol loading on net ecosystem CO 2
exchanges over different landscapes, Geophysical Research Letters, 31, 1–5, https://doi.org/10.1029/2004GL020915, 2004.

Nogueira, E. M., Nelson, B. W., Fearnside, P. M., França, M. B., and de Oliveira, Á. C. A.: Tree height in Brazil's 'arc of defor-
estation': Shorter trees in south and southwest Amazonia imply lower biomass, Forest Ecology and Management, 255, 2963–2972,
https://doi.org/10.1016/j.foreco.2008.02.002, 2008.

Oliveira, M. I., Acevedo, O. C., Sörgel, M., Nascimento, E. L., Manzi, A. O., Oliveira, P. E. S., Brondani, D. V., Tsokankunku, A., and
Andreae, M. O.: Planetary boundary layer evolution over the Amazon rainforest in episodes of deep moist convection at the Amazon Tall
Tower Observatory, Atmospheric Chemistry and Physics, 20, 15–27, https://doi.org/10.5194/acp-20-15-2020, 2020.

Oliveira, P. H., Artaxo, P., Pires, C., De Lucca, S., Procópio, A., Holben, B., Schafer, J., Cardoso, L. F., Wofsy, S. C., and Rocha, H. R.: The
effects of biomass burning aerosols and clouds on the CO2 flux in Amazonia, Tellus, Series B: Chemical and Physical Meteorology, 59,
338–349, https://doi.org/10.1111/j.1600-0889.2007.00270.x, 2007.

Oliveira-Filho AT, R. J. and Oliveira: The Cerrados of Brazil, vol. 20, Nova York, https://doi.org/10.1258/ijsa.2009.009019, 2002.

Ometto, J. and Kalaba, F.: CCP 7 Tropical Forests, https://doi.org/10.1017/9781009325844.024.2369, 2022.

Pan, Y.: A large and persistent carbon sink in the world's forests, Science, 333, 988–993, 2011.

Prado, D. E. and Gibbs, P. E.: Patterns of Species Distributions in the Dry Seasonal Forests of South America, Annals of the Missouri
Botanical Garden, 80, 902, https://doi.org/10.2307/2399937, 1993.

Procopio, A. S., Artaxo, P., Kaufman, Y. J., Remer, L. A., Schafer, J. S., and Holben, B. N.: Multiyear analysis of amazonian biomass burning
smoke radiative forcing of climate, Geophysical Research Letters, 31, 1–4, https://doi.org/10.1029/2003GL018646, 2004.

Rap, A.: Fires increase Amazon forest productivity, Geophysical Research Letters, pp. 4654–4662, https://doi.org/10.1002/2015GL063719.Received, 2015.

Rap, A., Scott, C. E., Reddington, C. L., Mercado, L., Ellis, R. J., Garraway, S., Evans, M. J., Beerling, D. J., MacKenzie, A. R., Hewitt, C. N., and Spracklen, D. V.: Enhanced global primary production by biogenic aerosol via diffuse radiation fertilization, Nature Geoscience, 11, 640–644, https://doi.org/10.1038/s41561-018-0208-3, 2018.

Ratter, J. A., Askew, G. P., Montgomery, R. F., and Gifford, D. R.: Observations on the vegetation of northeastern Mato Grosso II. Forests and soils of the Rio Suiá–Missu area., Proceedings of the Royal Society of London. Series B, Containing papers of a Biological character. Royal Society (Great Britain), 203, 191–208, https://doi.org/10.1098/rspb.1978.0100, 1978.

Reboita, M. S., Krusche, N., Ambrizzi, T., Porfírio, R., and Rocha, D.: Entendendo o Tempo e o Clima na América do Sul, Terra e Didatica, 8, 34–50, 2012.

Reichstein, M., Falge, E., Baldocchi, D., Papale, D., Aubinet, M., Berbigier, P., Bernhofer, C., Buchmann, N., Gilmanov, T., Granier, A., Grünwald, T., Havránková, K., Ilvesniemi, H., Janous, D., Knohl, A., Laurila, T., Lohila, A., Loustau, D., Matteucci, G., Meyers, T., Miglietta, F., Ourcival, J.-M., Pumpanen, J., Rambal, S., Rotenberg, E., Sanz, M., Tenhunen, J., Seufert, G., Vaccari, F., Vesala, T., Yakir, D., and Valentini, R.: On the separation of net ecosystem exchange into assimilation and ecosystem respiration: review and improved algorithm, Global Change Biology, 11, 1424–1439, https://doi.org/https://doi.org/10.1111/j.1365-2486.2005.001002.x, 2005.

Reindl, D., Beckman, W., and Duffie, J.: Diffuse fraction correlations, Solar Energy, 45, 1–7, https://doi.org/https://doi.org/10.1016/0038-092X(90)90060-P, 1990.

Remer, L. A., Kaufman, Y. J., Tanré, D., Mattoo, S., Chu, D. A., Martins, J. V., Li, R. R., Ichoku, C., Levy, R. C., Kleidman, R. G., Eck, T. F., Vermote, E., and Holben, B. N.: The MODIS aerosol algorithm, products, and validation, Journal of the Atmospheric Sciences, 62, 947–973, https://doi.org/10.1175/JAS3385.1, 2005.

Remer, L. A., Mattoo, S., Levy, R. C., and Munchak, L. A.: MODIS 3 km aerosol product: Algorithm and global perspective, Atmospheric Measurement Techniques, 6, 1829–1844, https://doi.org/10.5194/amt-6-1829-2013, 2013.

Saatchi, S., Longo, M., Xu, L., Yang, Y., Abe, H., André, M., Aukema, J. E., Carvalhais, N., Cadillo-Quiroz, H., Cerbu, G. A., Chernela, J. M., Covey, K., Sánchez-Clavijo, L. M., Cubillos, I. V., Davies, S. J., De Sy, V., De Vleeschouwer, F., Duque, A., Sybille Durieux, A. M., De Avila Fernandes, K., Fernandez, L. E., Gammino, V., Garrity, D. P., Gibbs, D. A., Gibbon, L., Gowae, G. Y., Hansen, M., Lee Harris, N., Healey, S. P., Hilton, R. G., Johnson, C. M., Kankeu, R. S., Laporte-Goetz, N. T., Lee, H., Lovejoy, T., Lowman, M., Lumbuenamo, R., Malhi, Y., Albert Martinez, J. M. M., Nobre, C., Pellegrini, A., Radachowsky, J., Román, F., Russell, D., Sheil, D., Smith, T. B., Spencer, R. G., Stolle, F., Tata, H. L., Torres, D. d. C., Tshimanga, R. M., Vargas, R., Venter, M., West, J., Widayati, A., Wilson, S. N., Brumby, S., and Elmore, A. C.: Detecting vulnerability of humid tropical forests to multiple stressors, One Earth, 4, 988–1003, https://doi.org/10.1016/j.oneear.2021.06.002, 2021.

Saatchi, S. S., Harris, N. L., Brown, S., Lefsky, M., Mitchard, E. T., Salas, W., Zutta, B. R., Buermann, W., Lewis, S. L., Hagen, S., Petrova, S., White, L., Silman, M., and Morel, A.: Benchmark map of forest carbon stocks in tropical regions across three continents, Proceedings of the National Academy of Sciences of the United States of America, 108, 9899–9904, https://doi.org/10.1073/pnas.1019576108, 2011.

Schafer, J. S., Eck, T. F., Holben, B. N., Artaxo, P., Yamasoe, M. A., and Procopio, A. S.: Observed reductions of total solar irradiance by biomass-burning aerosols in the Brazilian Amazon and Zambian Savanna, Geophysical Research Letters, 29, 2–5, https://doi.org/10.1029/2001GL014309, 2002a.

Schafer, J. S., Holben, B. N., Eck, T. F., Yamasoe, M. A., and Artaxo, P.: Atmospheric effects on insolation in the Brazilian Amazon: Observed modification of solar radiation by clouds and smoke and derived single scattering albedo of fire aerosols, Journal of Geophysical Research: Atmospheres, 107, LBA 41–1–LBA 41–15, https://doi.org/10.1029/2001JD000428, 2002b.

Schafer, J. S., Eck, T. F., Holben, B. N., Artaxo, P., and Duarte, A. F.: Characterization of the optical properties of atmospheric aerosols in Amazônia from long-term AERONET monitoring (1993-1995 and 1999-2006), Journal of Geophysical Research Atmospheres, 113, 1–16, https://doi.org/10.1029/2007JD009319, 2008.

Schuepp, P. H., Leclerc, M. Y., MacPherson, J. I., and Desjardins, R. L.: Footprint prediction of scalar fluxes from analytical solutions of the diffusion equation, Boundary-Layer Meteorology, 50, 355–373, https://doi.org/10.1007/BF00120530, 1990.

Shilling, J. E., Pekour, M. S., Fortner, E. C., Artaxo, P., de Sá, S., Hubbe, J. M., Longo, K. M., Machado, L. A. T., Martin, S. T., Springston, S. R., Tomlinson, J., and Wang, J.: Aircraft observations of the chemical composition and aging of aerosol in the Manaus urban plume during GoAmazon 2014/5, Atmospheric Chemistry and Physics, 18, 10 773–10 797, https://doi.org/10.5194/acp-18-10773-2018, 2018.

Silva Junior, C., O C Aragão, L. E., Anderson, L. O., Fonseca, M. G., Shimabukuro, Y. E., Vancutsem, C., Achard, F., Beuchle, R., Numata, I., Silva, C. A., Maeda, E. E., Longo, M., and Saatchi, S. S.: Persistent collapse of biomass in Amazonian forest edges following deforestation leads to unaccounted carbon losses, Tech. rep., http://advances.sciencemag.org/, 2020.

Spitters, C. J., Toussaint, H. A., and Goudriaan, J.: Separating the diffuse and direct component of global radiation and its implications for modeling canopy photosynthesis Part I. Components of incoming radiation, Agricultural and Forest Meteorology, 38, 217–229, https://doi.org/10.1016/0168-1923(86)90060-2, 1986.

Sullivan, M. J. P., Lewis, S. L., Affum-Baffoe, K., Castilho, C., Costa, F., Sanchez, A. C., Ewango, C. E. N., Hubau, W., Marimon, B., Monteagudo-Mendoza, A., Qie, L., Sonké, B., Martinez, R. V., Baker, T. R., Brienen, R. J. W., Feldpausch, T. R., Galbraith, D., Gloor, M., Malhi, Y., Aiba, S.-I., Alexiades, M. N., Almeida, E. C., de Oliveira, E. A., Dávila, E. Á., Loayza, P. A., Andrade, A., Vieira, S. A., Aragão, L., Araujo-Murakami, A., Arets, E. J. M. M., Arroyo, L., Ashton, P., C., G. A., Baccaro, F. B., Banin, L. F., Baraloto, C., Camargo, P. B., Barlow, J., Barroso, J., Bastin, J.-F., Batterman, S. A., Beeckman, H., Begne, S. K., Bennett, A. C., Berenguer, E., Berry, N., Blanc, L., Boeckx, P., Bogaert, J., Bonal, D., Bongers, F., Bradford, M., Brearley, F. Q., Brncic, T., Brown, F., Burban, B., Camargo, J. L., Castro, W., Céron, C., Ribeiro, S. C., Moscoso, V. C., Chave, J., Chezeaux, E., Clark, C. J., de Souza, F. C., Collins, M., Comiskey, J. A., Valverde, F. C., Medina, M. C., da Costa, L., Danˇcák, M., Dargie, G. C., Davies, S., Cardozo, N. D., Thales de Haulleville, de Medeiros, M. B., Pasquel, J. d. A., Derroire, G., Fiore, A. D., Doucet, J.-L., Dourdain, A., Droissart, V., Duque, L. F., Ekoungoulou, R., Elias, F., Erwin, T., Esquivel-Muelbert, A., Fauset, S., Ferreira, J., Llampazo, G. F., Foli, E., Ford, A., Gilpin, M., Hall, J. S., Hamer, K. C., Hamilton, A. C., Harris, D. J., Hart, T. B., Hédl, R., Herault, B., Herrera, R., Higuchi, N., Hladik, A., Eurídice Honorio Coronado, Huamantupa-Chuquimaco, I., Huasco, W. H., Jeffery, K. J., Jimenez-Rojas, E., Kalamandeen, M., Kamdem, M.-N., Kearsley, E., Umetsu, R. K., Khoon, L. K. K., Killeen, T., Kitayama, K., Klitgaard, B., Koch, A., Labrière, N., Laurance, W., Laurance, S., Leal, M. E., Levesley, A., Lima, A. J. N., Lisingo, J., Pontes-Lopes, A., Lopez-Gonzalez, G., Lovejoy, T., Lovett, J., Lowe, R., Magnusson, W. E., Malumbres-Olarte, J., Manzatto, Â. G., Jr., B. H. M., Marshall, A. R., Marthews, T., Reis, S. M. d. A., Maycock, C., Melgaço, K., Mendoza, C., Metali, F., Mihindou, V., Milliken, W., Mitchard, E., Morandi, P. S., Mossman, H. L., Nagy, L., Nascimento, H., Neill, D., Nilus, R., Vargas, P. N., Palacios, W., Camacho, N. P., Peacock, J., Pendry, C., Mora, M. C. P., Pickavance, G. C., Pipoly, J., Pitman, N., Playfair, M., Poorter, L., Poulsen, J. R., Poulsen, A. D., Preziosi, R., Prieto, A., Richard Primack, Ramírez-Angulo, H., Reitsma, J., Réjou-Méchain, M., Correa, Z. R., de Sousa, T. R., Bayona, L. R., Roopsind, A., Rudas, A., Rutishauser, E., Salim, K. A., Salomão, R. P., Schietti, J., Sheil, D., Silva, R. C., Espejo, J. S., Valeria, C. S., Silveira, M., Simo-Droissart, M., Simon, M. F., Singh, J., Shareva, Y. C. S., Stahl, C., Stropp, J., Sukri, R., Sunderland, T., Svátek, M., Swaine, M. D., Swamy, V., Taedoumg, H., Talbot, J., James Taplin, Taylor, D., ter Steege, H., Terborgh,

J., Thomas, R., Thomas, S. C., Torres-Lezama, A., Umunay, P., Gamarra, L. V., van der Heijden, G., van der Hout, P., van der Meer, P. J., van Nieuwstadt, M., Verbeeck, H., Vernimmen, R., Vicentini, A., Vieira, I. C. G., Torre, E. V., Vleminckx, J., Vos, V. A., Wang, O., White, L. J. T., Willcock, S., Woods, J. T., Wortel, V., Young, K., Zagt, R., Zemagho, L., Zuidema, P. A., Zwerts, J. A., and Phillips, O. L.: Long-term thermal sensitivity of Earth's tropical forests, Science, in press, 869–874, 2020.

1000 Tribuzy, E. S.: Canopy leaf temperature variations and their effect on the CO2 assimilation rate in Central Amazonia (in Portuguese), Doctoral thesis, p. 102, 2005.

Venturini, A. M., Gontijo, J. B., Mandro, J. A., Berenguer, E., Peay, K. G., Tsai, S. M., and Bohannan, B. J. M.: Soil microbes under threat in the Amazon Rainforest, Tech. rep., 2023.

von Randow, C., Manzi, A. O., Kruijt, B., de Oliveira, P. J., Zanchi, F. B., Silva, R. L., Hodnett, M. G., Gash, J. H., Elbers, J. A., Waterloo, 1005 M. J., Cardoso, F. L., and Kabat, P.: Comparative measurements and seasonal variations in energy and carbon exchange over forest and pasture in South West Amazonia, Theoretical and Applied Climatology, 78, 5–26, https://doi.org/10.1007/s00704-004-0041-z, 2004.

Vourlitis, G. L., Priante Filho, N., Hayashi, M. M., Nogueira, J. D. S., Caseiro, F. T., and Holanda Campelo, J.: Seasonal variations in the net ecosystem CO2 exchange of a mature Amazonian transitional tropical forest (cerradão), Functional Ecology, 15, 388–395, https://doi.org/10.1046/j.1365-2435.2001.00535.x, 2001.

1010 Vourlitis, G. L., Priante Filho, N., Hayashi, M. M., Nogueira, J. D. S., Caseiro, F. T., and Campelo, J. H.: Seasonal variations in the evapotranspiration of a transitional tropical forest of Mato Grosso, Brazil, Water Resources Research, 38, 30–1–30–11, https://doi.org/10.1029/2000wr000122, 2002.

Vourlitis, G. L., De Almeida Lobo, F., Zeilhofer, P., and De Souza Nogueira, J.: Temporal patterns of net CO2 exchange for a tropical semideciduous forest of the southern Amazon Basin, Journal of Geophysical Research: Biogeosciences, 116, 1–15, 1015 https://doi.org/10.1029/2010JG001524, 2011.

Wang, X., Wang, C., Wu, J., Miao, G., Chen, M., Chen, S., Wang, S., Guo, Z., Wang, Z., Wang, B., Li, J., Zhao, Y., Wu, X., Zhao, C., Lin, W., Zhang, Y., and Liu, L.: Intermediate Aerosol Loading Enhances Photosynthetic Activity of Croplands, Geophysical Research Letters, 48, e2020GL091 893, https://doi.org/https://doi.org/10.1029/2020GL091893, e2020GL091893 2020GL091893, 2021.

Wang, Z., Wang, C., Wang, X., Wang, B., Wu, J., and Liu, L.: Aerosol pollution alters the diurnal dynamics of sun and shade leaf pho- 1020 tosynthesis through different mechanisms, Plant, Cell & Environment, 45, 2943–2953, https://doi.org/https://doi.org/10.1111/pce.14411, 2022.

Wu, J., Albert, L. P., Lopes, A. P., Restrepo-Coupe, N., Hayek, M., Wiedemann, K. T., Guan, K., Stark, S. C., Christoffersen, B., Prohaska, N., Tavares, J. V., Marostica, S., Kobayashi, H., Ferreira, M. L., Campos, K. S., da Silva, R., Brando, P. M., Dye, D. G., Huxman, T. E., Huete, A. R., Nelson, B. W., and Saleska, S. R.: Leaf development and demography explain photosynthetic seasonality in Amazon evergreen 1025 forests, Science, 351, 972–976, https://doi.org/10.1126/science.aad5068, 2016.

Wutzler, T., Lucas-Moffat, A., Migliavacca, M., Knauer, J., Sickel, K., Šigut, L., Menzer, O., and Reichstein, M.: Basic and extensible post-processing of eddy covariance flux data with REddyProc, Biogeosciences, 15, 5015–5030, https://doi.org/10.5194/bg-15-5015-2018, 2018.

Yakir, D.: 4.07 - The Stable Isotopic Composition of Atmospheric CO2, in: Treatise on Geochemistry, edited by Holland, H. D. and Turekian, 1030 K. K., pp. 175–212, Pergamon, Oxford, https://doi.org/https://doi.org/10.1016/B0-08-043751-6/04038-X, 2003.

Yamasoe, M. A., Randow, C. V., Manzi, A. O., Schafer, J. S., Eck, T. F., and Holben, B. N.: Effect of smoke and clouds on the transmissivity of photosynthetically active radiation inside the canopy., pp. 1645–1656, 2006.

Yuan, W., Zheng, Y., Piao, S., Ciais, P., Lombardozzi, D., Wang, Y., Ryu, Y., Chen, G., Dong, W., Hu, Z., Jain, A. K., Jiang, C., Kato, E., Li, S., Lienert, S., Liu, S., Nabel, J. E., Qin, Z., Quine, T., Sitch, S., Smith, W. K., Wang, F., Wu, C., Xiao, Z., and Yang, S.: Increased atmospheric vapor pressure deficit reduces global vegetation growth, Science Advances, 5, 1–13, https://doi.org/10.1126/sciadv.aax1396, 2019.

Zhang, M., Yu, G. R., Zhang, L. M., Sun, X. M., Wen, X. F., Han, S. J., and Yan, J. H.: Impact of cloudiness on net ecosystem exchange of carbon dioxide in different types of forest ecosystems in China, Biogeosciences, 7, 711–722, https://doi.org/10.5194/bg-7-711-2010, 2010.

1035